reduced sensitivity to haloperidol in the Fyn-deficient mice is because of defective dopaminergic transmission.

We found that haloperidol increased phosphorylation of the Tyr-418 residues of Fyn. The catalytic activity of SFKs is controlled through autocatalytic phosphorylation and dephosphorylation, particularly at amino acid residues Tyr-418 and Tyr-529 (14), and the phosphorylated Tyr-529 intramolecularly interacts with an Src homology 2 domain to form a loop, thereby suppressing kinase function. Intermolecular autophosphorylation at Tyr-418, on the other hand, activates SFKs by displacing Tyr-418 from the substrate-binding site, thus allowing the kinase to gain access to substrates (33). We found that the haloperidol-induced increase in Tyr-418 phosphorylation occurred specifically in Fyn and did not occur in Src, whereas phosphorylation of Tyr-529 was the same in both Src and Fyn. Thus, Fyn is specifically activated by haloperidol *in vivo*.

Haloperidol also increased the phosphorylation of Tyr-1472 in the NR2B subunit, and because no increase was observed in Fyn-deficient mice, the haloperidol-induced phosphorylation of NR2B subunit must be dependent on Fyn. Moreover, we confirmed this D_2-R antagonist induced Fyn-mediated enhancement of NR2B phosphorylation at the cellular level in primary cultures of striatal neurons.

Fyn-mediated phosphorylation of NR2B and potentiation of NMDA-R channel activity are involved in several brain functions, including ethanol tolerance (15), seizure susceptibility (23), and long term potentiation (17). Activation of EphB receptors has also been reported to result in increased phosphorylation of NR2B and an increase in NMDA-R channel activity measured by Ca^{2+} imaging in hippocampal primary cultures (34). The use of HEK293T cells transfected with a mutant NR2B construct in this study also showed that Fyn-mediated tyrosine phosphorylation of NR2B is required for the increase in NMDA-R channel activity. In our study, NMDA-R channel activity in most wild-type striatal neurons was increased by the blockade of D_2-R, and the proportion of such neurons was significantly reduced in Fyn deficiency. Thus, the increased NMDA-R activity after D_2-R blockade in most of the striatal neurons was Fyn-dependent. However, NMDA-R may also be activated by a Fyn-independent pathway, because a certain proportion of the neurons in the Fyn-deficient striatal culture exhibited increased NMDA-R activity.

It has been repeatedly observed that the NMDA-R antagonist MK-801 attenuates haloperidol-induced catalepsy (9, 35–37), and we recently reported that prior exposure to the NR2B-selective antagonist CP-101,606 significantly reduces haloperidol-induced catalepsy (9). Thus, haloperidol-induced catalepsy is specifically dependent on NR2B function, and activation of NR2B function by Fyn-mediated phosphorylation is likely to be required for catalepsy to occur.

NMDA-R dysfunction is hypothesized to be the pathogenetic mechanism responsible for schizophrenia, because NMDA-R antagonists cause psychotic states resembling schizophrenia (38–40), and mice with reduced NMDA-R expression have been reported to display schizophrenia-related behaviors (41). Because unmedicated schizophrenic patients exhibit attenuated EPS shortly after haloperidol administration compared with healthy controls (42), the lower responsiveness to haloperidol in Fyn-deficient mice may mimic a feature of schizophrenia.

Several mutant mice, including mice deficient in the D_2-R (24), A_{2A}-adenosine receptor (43), retinoid X receptor γ1 (44), and protein kinase A (PKA) (45), show reduced cataleptic responses to haloperidol. The reduced cataleptic response in one of them, the PKA-deficient mutant, is likely to be caused by a molecular mechanism similar to that in Fyn deficiency, because an increase in PKA-mediated serine phosphorylation of striatal NR1 subunits increases following haloperidol administration (46). The scaffolding protein RACK1 binds to both Fyn and NR2B, and the three molecules form a complex in rat hippocampus (16, 47). Dissociation of RACK1 from this RACK1-Fyn-NR2B complex facilitates Fyn-mediated phosphorylation of NR2B (47). Because PKA activation has been demonstrated to dissociate RACK1 from this complex (16), the above PKA-RACK1-Fyn pathway may also exist downstream of D_2-R in the striatum.

Another molecule that may act between D_2-R and Fyn is PKC. Activation of G-protein-coupled receptors, such as muscarinic and metabotropic glutamate receptors, in the hippocampus increases NMDA-evoked currents via protein kinase C (PKC) (48). The increase in NMDA-R function is mediated by the activation of SFKs, because the PKC-induced NMDA-R up-regulation is blocked by an inhibitor of Src and Fyn and does not occur in Src-deficient cells (48). D_2-R is another G-protein-coupled receptor, and because haloperidol administration acutely increases PKC activity in the rat striatum (49), Fyn activation after D_2-R blockade may be mediated by the PKC pathway.

Other molecules, including receptor tyrosine kinases (34, 50) and a cytokine receptor (51), have also been reported to be involved in SFK-mediated phosphorylation and activation of NMDA-R, and they may be involved in the striatal activation of Fyn after D_2-R inhibition.

In this study we found that blockade of D_2-R causes Fyn activation, Fyn-mediated NMDA-R phosphorylation, and potentiation of its channel activity in the striatal neurons that may be responsible for haloperidol-induced catalepsy. Further investigation should focus on the above-postulated Fyn-activation mechanisms initiated by D_2-R blockade, and these transduction steps should be drug targets for controlling not only motor function but higher cognitive brain function.

Acknowledgments—We are grateful to Dr. H. Niki (Brain Science Institute, RIKEN, Japan) for reading the manuscript and giving us invaluable advice. We are also grateful to Dr. T. Kaneko (Kyoto University) for the gift of the mouse dopamine D_2 receptor cDNA, Dr. M. Watanabe (Hokkaido University) for the gift of the anti-NR2B antibody, and Prof. N. Koshikawa (Department of Pharmacology, Nihon University School of Dentistry) for helpful advice on the determination of muscular rigidity. We also thank K. Kamimura and T. Muto (Department of Anatomy and Developmental Biology, Chiba University Graduate School of Medicine) for their technical assistance in the immunohistochemistry and behavioral analyses.

REFERENCES

1. Crocker, A. D., and Hemsley, K. M. (2001) *Prog. Neuropsychopharmacol. Biol. Psychiatry* **25,** 573–590
2. Wadenberg, M. L., Soliman, A., VanderSpek, S. C., and Kapur, S. (2001) *Neuropsychopharmacology* **25,** 633–641
3. Moore, N. A., Blackman, A., Awere, S., and Leander, J. D. (1993) *Eur. J. Pharmacol.* **237,** 1–7
4. Chartoff, E. H., Ward, R. P., and Dorsa, D. M. (1999) *J. Pharmacol. Exp. Ther.* **291,** 531–537
5. Chase, T. N. (2004) *Parkinsonism Relat. Disord.* **10,** 305–313
6. Sucher, N. J., Awobuluyi, M., Choi, Y. B., and Lipton, S. A. (1996) *Trends Pharmacol. Sci.* **17,** 348–355
7. Standaert, D. G., Testa, C. M., Young, A. B., and Penney, J. B., Jr. (1994) *J. Comp. Neurol.* **343,** 1–16
8. Kosinski, C. M., Standaert, D. G., Counihan, T. J., Scherzer, C. R., Kerner, J. A., Daggett, L. P., Velicelebi, G., Penney, J. B., Young, A. B., and Landwehrmeyer, G. B. (1998) *J. Comp. Neurol.* **390,** 63–74
9. Yanahashi, S., Hashimoto, K., Hattori, K., Yuasa, S., and Iyo, M. (2004) *Brain Res.* **1011,** 84–93
10. Wang, Y. T., and Salter, M. W. (1994) *Nature* **369,** 233–235
11. Tingley, W. G., Ehlers, M. D., Kameyama, K., Doherty, C., Ptak, J. B., Riley, C. T., and Huganir, R. L. (1997) *J. Biol. Chem.* **272,** 5157–5166
12. Menegoz, M., Lau, L. F., Herve, D., Huganir, R. L., and Girault, J. A. (1995) *Neuroreport* **7,** 125–128
13. Oh, J. D., Russell, D. S., Vaughan, C. L., Chase, T. N., and Russell, D. (1998) *Brain Res.* **813,** 150–159

14. Salter, M. W., and Kalia, L. V. (2004) *Nat. Rev. Neurosci.* **5,** 317–328
15. Miyakawa, T., Yagi, T., Kitazawa, H., Yasuda, M., Kawai, N., Tsuboi, K., and Niki, H. (1997) *Science* **278,** 698–701
16. Yaka, R., Phamluong, K., and Ron, D. (2003) *J. Neurosci.* **23,** 3623–3632
17. Nakazawa, T., Komai, S., Tezuka, T., Hisatsune, C., Umemori, H., Semba, K., Mishina, M., Manabe, T., and Yamamoto, T. (2001) *J. Biol. Chem.* **276,** 693–699
18. Kojima, N., Ishibashi, H., Obata, K., and Kandel, E. R. (1998) *Learn. Mem.* **5,** 429–445
19. Cheung, H. H., and Gurd, J. W. (2001) *J. Neurochem.* **78,** 524–534
20. Yagi, T., Shigetani, Y., Okado, N., Tokunaga, T., Ikawa, Y., and Aizawa, S. (1993) *Oncogene* **8,** 3343–3351
21. Kulagowski, J. J., Broughton, H. B., Curtis, N. R., Mawer, I. M., Ridgill, M. P., Baker, R., Emms, F., Freedman, S. B., Marwood, R., Patel, S., Ragan, C. I., and Leeson, P. D. (1996) *J. Med. Chem.* **39,** 1941–1942
22. Watanabe, M., Fukaya, M., Sakimura, K., Manabe, T., Mishina, M., and Inoue, Y. (1998) *Eur. J. Neurosci.* **10,** 478–487
23. Yasunaga, M., Yagi, T., Hanzawa, N., Yasuda, M., Yamanashi, Y., Yamamoto, T., Aizawa, S., Miyauchi, Y., and Nishikawa, S. (1996) *J. Cell Biol.* **132,** 91–99
24. Boulay, D., Depoortere, R., Oblin, A., Sanger, D. J., Schoemaker, H., and Perrault, G. (2000) *Eur. J. Pharmacol.* **391,** 63–73
25. Lorenc-Koci, E., Wolfarth, S., and Ossowska, K. (1996) *Exp. Brain Res.* **109,** 268–276
26. Yuasa, S. (1996) *Anat. Embryol.* **194,** 223–234
27. Uchino, S., Watanabe, W., Nakamura, T., Shuto, S., Kazuta, Y., Matsuda, A., Nakajima-Iijima, S., Kudo, Y., Kohsaka, S., and Mishina, M. (2001) *FEBS Lett.* **506,** 117–122
28. Cepeda, C., Buchwald, N. A., and Levine, M. S. (1993) *Proc. Natl. Acad. Sci. U. S. A.* **90,** 9576–9580
29. Millan, M. J., Dekeyne, A., Rivet, J. M., Dubuffet, T., Lavielle, G., and Brocco, M. (2000) *J. Pharmacol. Exp. Ther.* **293,** 1063–1073
30. Miyakawa, T., Yagi, T., Kagiyama, A., and Niki, H. (1996) *Brain Res. Mol. Brain Res.* **37,** 145–150
31. Miyakawa, T., Yagi, T., Watanabe, S., and Niki, H. (1994) *Brain Res. Mol. Brain Res.* **27,** 179–182
32. Hironaka, N., Yagi, T., and Niki, H. (2002) *Brain Res. Mol. Brain Res.* **98,** 102–110
33. Xu, W., Doshi, A., Lei, M., Eck, M. J., and Harrison, S. C. (1999) *Mol. Cell* **3,** 629–638
34. Takasu, M. A., Dalva, M. B., Zigmond, R. E., and Greenberg, M. E. (2002) *Science* **295,** 491–495
35. de Souza, I. E., and Meredith, G. E. (1999) *Synapse* **32,** 243–253
36. Dragunow, M., Robertson, G. S., Faull, R. L., Robertson, H. A., and Jansen, K. (1990) *Neuroscience* **37,** 287–294
37. Ziolkowska, B., and Hollt, V. (1993) *Neurosci. Lett.* **156,** 39–42
38. Olney, J. W., and Farber, N. B. (1995) *Arch. Gen. Psychiatry* **52,** 998–1007
39. Tsai, G., and Coyle, J. T. (2002) *Annu. Rev. Pharmacol. Toxicol.* **42,** 165–179
40. Svensson, T. H. (2000) *Brain Res. Brain Res. Rev.* **31,** 320–329
41. Mohn, A. R., Gainetdinov, R. R., Caron, M. G., and Koller, B. H. (1999) *Cell* **98,** 427–436
42. Miller, A. L., Maas, J. W., Contreras, S., Seleshi, E., True, J. E., Bowden, C., and Castiglioni, J. (1993) *Biol. Psychiatry* **34,** 178–187
43. Chen, J. F., Moratalla, R., Impagnatiello, F., Grandy, D. K., Cuellar, B., Rubinstein, M., Beilstein, M. A., Hackett, E., Fink, J. S., Low, M. J., Ongini, E., and Schwarzschild, M. A. (2001) *Proc. Natl. Acad. Sci. U. S. A.* **98,** 1970–1975
44. Saga, Y., Kobayashi, M., Ohta, H., Murai, N., Nakai, N., Oshima, M., and Taketo, M. M. (1999) *Genes Cells* **4,** 219–228
45. Adams, M. R., Brandon, E. P., Chartoff, E. H., Idzerda, R. L., Dorsa, D. M., and McKnight, G. S. (1997) *Proc. Natl. Acad. Sci. U. S. A.* **94,** 12157–12161
46. Leveque, J. C., Macias, W., Rajadhyaksha, A., Carlson, R. R., Barczak, A., Kang, S., Li, X. M., Coyle, J. T., Huganir, R. L., Heckers, S., and Konradi, C. (2000) *J. Neurosci.* **20,** 4011–4020
47. Yaka, R., Thornton, C., Vagts, A. J., Phamluong, K., Bonci, A., and Ron, D. (2002) *Proc. Natl. Acad. Sci. U. S. A.* **99,** 5710–5715
48. Lu, W. Y., Xiong, Z. G., Lei, S., Orser, B. A., Dudek, E., Browning, M. D., and MacDonald, J. F. (1999) *Nat. Neurosci.* **2,** 331–338
49. Dwivedi, Y., and Pandey, G. N. (1999) *J. Pharmacol. Exp. Ther.* **291,** 688–704
50. Kotecha, S. A., Oak, J. N., Jackson, M. F., Perez, Y., Orser, B. A., Van Tol, H. H., and MacDonald, J. F. (2002) *Neuron* **35,** 1111–1122
51. Viviani, B., Bartesaghi, S., Gardoni, F., Vezzani, A., Behrens, M. M., Bartfai, T., Binaglia, M., Corsini, E., Di Luca, M., Galli, C. L., and Marinovich, M. (2003) *J. Neurosci.* **23,** 8692–8700

International weekly journal of science

nature

UDP acting at $P2Y_6$ receptors is a mediator of microglial phagocytosis

Schuichi Koizumi[1,2*], Yukari Shigemoto-Mogami[1*], Kaoru Nasu-Tada[1], Yoichi Shinozaki[1,3], Keiko Ohsawa[4], Makoto Tsuda[3], Bhalchandra V. Joshi[5], Kenneth A. Jacobson[5], Shinichi Kohsaka[4] & Kazuhide Inoue[3]

[1]Division of Pharmacology, National Institute of Health Sciences, 1-18-1 Kamiyoga, Setagaya, Tokyo 158-8501, Japan. [2]Department of Pharmacology, Interdisciplinary Graduate School of Medicine and Engineering, University of Yamanashi, 1110 Shimokato, Chuo, Yamanashi 409-3893, Japan. [3]Department of Molecular and SystemPharmacology, Graduate School of Pharmaceutical Sciences, Kyushu University, 3-1-1 Maidashi, Higashi, Fukuoka 812-8582, Japan. [4]Department of Neurochemistry, National Institute of Neuroscience, 4-1-1 Ogawahigashi, Kodaira, Tokyo 187-8502, Japan. [5]Molecular Recognition Section, Laboratory of Bioorganic Chemistry, National Institute of Diabetes and Digestive and Kidney Diseases, National Institutes of Health, Bethesda, Maryland 20892-0810, USA.

**These authors contributed equally to this work.*

Reprinted from Nature, Vol. 446, No. 7139, pp. 1091–1095, 26 April 2007

Vol 446|26 April 2007|doi:10.1038/nature05704

LETTERS

UDP acting at $P2Y_6$ receptors is a mediator of microglial phagocytosis

Schuichi Koizumi[1,2*], Yukari Shigemoto-Mogami[1*], Kaoru Nasu-Tada[1], Yoichi Shinozaki[1,3], Keiko Ohsawa[4], Makoto Tsuda[3], Bhalchandra V. Joshi[5], Kenneth A. Jacobson[5], Shinichi Kohsaka[4] & Kazuhide Inoue[3]

Microglia, brain immune cells, engage in the clearance of dead cells or dangerous debris, which is crucial to the maintenance of brain functions. When a neighbouring cell is injured, microglia move rapidly towards it or extend a process to engulf the injured cell. Because cells release or leak ATP when they are stimulated[1,2] or injured[3,4], extracellular nucleotides are thought to be involved in these events. In fact, ATP triggers a dynamic change in the motility of microglia *in vitro*[5,6] and *in vivo*[3,4], a previously unrecognized mechanism underlying microglial chemotaxis[5,6]; in contrast, microglial phagocytosis has received only limited attention. Here we show that microglia express the metabotropic $P2Y_6$ receptor whose activation by endogenous agonist UDP triggers microglial phagocytosis. UDP facilitated the uptake of microspheres in a $P2Y_6$-receptor-dependent manner, which was mimicked by the leakage of endogenous UDP when hippocampal neurons were damaged by kainic acid *in vivo* and *in vitro*. In addition, systemic administration of kainic acid in rats resulted in neuronal cell death in the hippocampal CA1 and CA3 regions, where increases in messenger RNA encoding $P2Y_6$ receptors that colocalized with activated microglia were observed. Thus, the $P2Y_6$ receptor is upregulated when neurons are damaged, and could function as a sensor for phagocytosis by sensing diffusible UDP signals, which is a previously unknown pathophysiological function of P2 receptors in microglia.

Microglia express several functional P2 receptors, and their $P2X_4$, $P2X_7$ and $P2Y_{12}$ receptors have already been described in relation to their physiological and pathophysiological consequences[5–9]. To investigate the expression of mRNAs for P2 receptors that are at a higher concentration in cultured rat microglia, we conducted reverse-transcriptase-mediated polymerase chain reaction (RT–PCR) analysis with complementary DNA coding for P2Y and P2X receptors (Fig. 1a). In accordance with previous reports[5–9], microglia expressed mRNAs encoding $P2X_4$, $P2X_7$ and $P2Y_{12}$ receptors. However, we found unexpectedly that cultured rat microglia expressed a large amount of mRNA coding for $P2Y_6$ receptors, which was also confirmed by western blotting for the expression of $P2Y_6$ receptor protein (Fig. 1b). The $P2Y_6$ receptor is coupled to the activation of phospholipase C (PLC), leading to the production of inositol 1,4,5-trisphosphate ($InsP_3$) and the release of Ca^{2+} from $InsP_3$-receptor-sensitive stores[10,11]. We therefore examined changes in the intracellular Ca^{2+} concentration ($[Ca^{2+}]_i$) in microglia and found that the $P2Y_6$ receptor agonist UDP evoked increases in $[Ca^{2+}]_i$ in a concentration-dependent manner, and it also increased the fraction of the UDP-responsive cells (Supplementary Fig. 1a). The elevations in $[Ca^{2+}]_i$ induced by 100 μM UDP were significantly inhibited by the PLC inhibitor U73122, the Ca^{2+}-ATPase inhibitor in sarcoplasmic/endoplasmic reticulum thapsigargin, and the membrane-permeable $InsP_3$ receptor inhibitor xestospongin C, but were little affected by pertussis toxin (Supplementary Fig. 1b). The UDP-evoked $[Ca^{2+}]_i$ increases in microglia were significantly inhibited by reactive blue 2 (RB2), known as a potent $P2Y_6$ antagonist[11], suramin, which inhibits $P2Y_6$ receptor at higher concentrations, the diisothiocyanate derivative MRS2578, which is a selective antagonist of the $P2Y_6$ receptor[12], and an antisense oligonucleotide (AS) for $P2Y_6$ receptors, but not by a random-sequence oligonucleotide (R-oligo) (Fig. 1c). All these data show that rat microglia express functional $P2Y_6$ receptors by which UDP mobilizes Ca^{2+}.

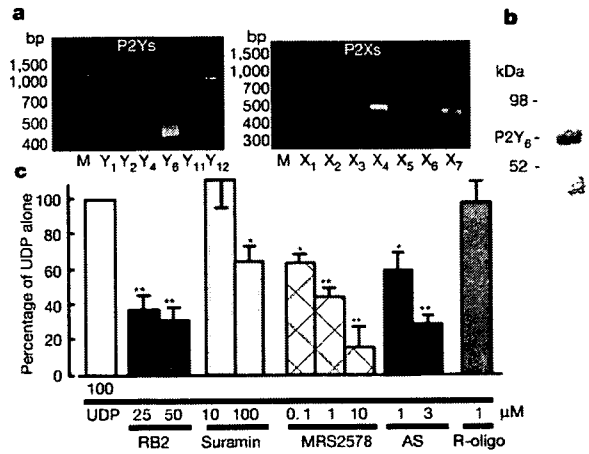

Figure 1 | Expression of $P2Y_6$ receptor and UDP-evoked increase in $[Ca^{2+}]_i$ in cultured microglia. a, RT–PCR analysis of the expression of mRNAs for $P2Y_6$, $P2Y_{12}$, $P2X_4$ and $P2X_7$ receptors in microglial cells. **b**, Expression of $P2Y_6$ receptor protein confirmed by western blotting analysis. **c**, Effects of various chemicals on the increase in $[Ca^{2+}]_i$ (measured as the change in ratio of fluorescence at 340 nm to that at 380 nm) evoked by 100 μM UDP in microglia. The maximum increase in Fura-2 fluorescence evoked by 100 μM UDP was considered as the control response, and values are expressed as a percentage of control. Data show means and s.e.m. for 24–36 cells obtained from at least three independent experiments. Significant differences from the response to UDP alone: asterisk, $P < 0.05$; two asterisks, $P < 0.01$ (Student's *t*-test).

[1]Division of Pharmacology, National Institute of Health Sciences, 1-18-1 Kamiyoga, Setagaya, Tokyo 158-8501, Japan. [2]Department of Pharmacology, Interdisciplinary Graduate School of Medicine and Engineering, University of Yamanashi, 1110 Shimokato, Chuo, Yamanashi 409-3893, Japan. [3]Department of Molecular and System Pharmacology, Graduate School of Pharmaceutical Sciences, Kyushu University, 3-1-1 Maidashi, Higashi, Fukuoka 812-8582, Japan. [4]Department of Neurochemistry, National Institute of Neuroscience, 4-1-1 Ogawahigashi, Kodaira, Tokyo 187-8502, Japan. [5]Molecular Recognition Section, Laboratory of Bioorganic Chemistry, National Institute of Diabetes and Digestive and Kidney Diseases, National Institutes of Health, Bethesda, Maryland 20892-0810, USA.
*These authors contributed equally to this work.

Morphogenesis, cell movement and phagocytosis are driven by dynamic reorganization of the actin cytoskeleton[13,14]. We showed previously that activation of $P2Y_{12/13}$ receptors, another microglial G-protein-coupled receptor, resulted in membrane ruffling and chemotaxis in microglia[5,6], and therefore we sought first to determine whether the $P2Y_6$-receptor-mediated signals affect the cell movement of microglia. Membrane ruffles are structures that are found primarily at the front edges of migrating cells[15]. To determine whether $P2Y_6$ activation stimulates microglial chemotaxis, cells were stimulated with either UDP or ATP. Neither lamellipodia-like membrane ruffles (Fig. 2a left) nor chemotaxis (Fig. 2b left) were observed when stimulated with UDP, whereas ATP produced both responses (Fig. 2a right and Fig. 2b right). However, UDP caused actin reorganization and formed aggregates of F-actin in the interior of the cells (Fig. 2a left, arrows). On stimulation with UDP (100 μM), microglia rapidly changed their morphology (Supplementary Fig. 2a); namely, to microglial processes with filopodia-like protrusions (arrows) and phagosome-like vacuoles (arrowheads). A crown-like circular structure rich in F-actins, termed the 'phagocytotic cup'[16], was also observed around the zymosan particles (Supplementary Fig. 2b, red). We speculated that UDP somehow regulates the morphogenesis of microglia, which may be involved in microglial endocytotic activities such as pinocytosis, macropinocytosis and phagocytosis. Phagocytosis is one of the most important physiological functions of microglia[17] and is the process activating the uptake of larger particles (more than 0.5 μm) by actin-based mechanisms. We investigated the UDP-evoked phagocytosis process by time-lapse videomicroscopy and flow cytometry (fluorescence-activated cell sorting; FACS)-based assay. When stimulated with 100 μM UDP, microglia rapidly phagocytosed fluorescent zymosan particles (green) (Fig. 2c, see also Supplementary Video). A quantitative phagocytosis assay by FACS shows that UDP induced the phagocytosis of latex beads in a concentration-dependent fashion (5–1,000 μM) in a 20-min incubation period (Fig. 2d). GDP (100–1,000 μM), a weak agonist of the $P2Y_6$ receptor, caused a slight uptake of microspheres (at 100 μM this was 49.7 ± 8.6% of UDP alone; $n = 4$) but ADP, also known as a weak partial agonist of the mouse $P2Y_6$ receptor, failed to stimulate the uptake (at 100 μM it was 0.3 ± 2.3% of UDP alone; $n = 4$). This is in good agreement with the previous finding that ADP does not activate rat $P2Y_6$ receptors[18]. The phagocytosis induced by 100 μM UDP was significantly inhibited by 30–100 μM RB2, a higher concentration of suramin (300 μM) and MRS2578 (0.01–3 μM), and was nearly abolished by $P2Y_6$ AS (Fig. 2e; see also Supplementary Fig. 2c, d). Recent reports indicate the existence of functional cross-talk between the nucleotides and cysteinyl leukotrienes (CysLTs, for example LTD4) in orchestrating inflammatory responses[19], indicating that some nucleotides may reveal their functions by means of a CysLT receptor (CysLTR). Microglia express a functional CysLT1R, whose activation by LTD4 resulted in an increase in $[Ca^{2+}]_i$ in microglia (Supplementary Fig. 3a). Thus, UDP acting on CysLT1R may reveal various microglial responses. However, MRS2578, a selective $P2Y_6$ receptor antagonist, did not block the LTD4-evoked Ca^{2+} responses in CysLT1R-transfected Chinese hamster ovary cells (Supplementary Fig. 3b) at a dose that inhibited the UDP-evoked increase in $[Ca^{2+}]_i$ and phagocytosis in microglia (Figs 1c and 2e). In addition, 1 μM LTD4 did not induce phagocytosis in microglia (Supplementary Fig. 3c, 4.8 ± 4.2% of that with 100 μM UDP alone; $n = 3$). All these findings suggest that the contribution of the CysLT1R to the UDP-evoked phagocytosis in microglia is negligible. Taken together, these data strongly suggest that rat microglial $P2Y_6$ receptors are coupled with phagocytic functions. The UDP-evoked phagocytosis was inhibited by 1 μM thapsigargin, the protein kinase C inhibitor staurosporin at 5 μM, and 10 μM U73122 (see Supplementary Fig. 4), indicating that activation of the $P2Y_6$ receptor seems to trigger phagocytosis through the pathway(s) mediated by PLC-linked Ca^{2+} and protein kinase C.

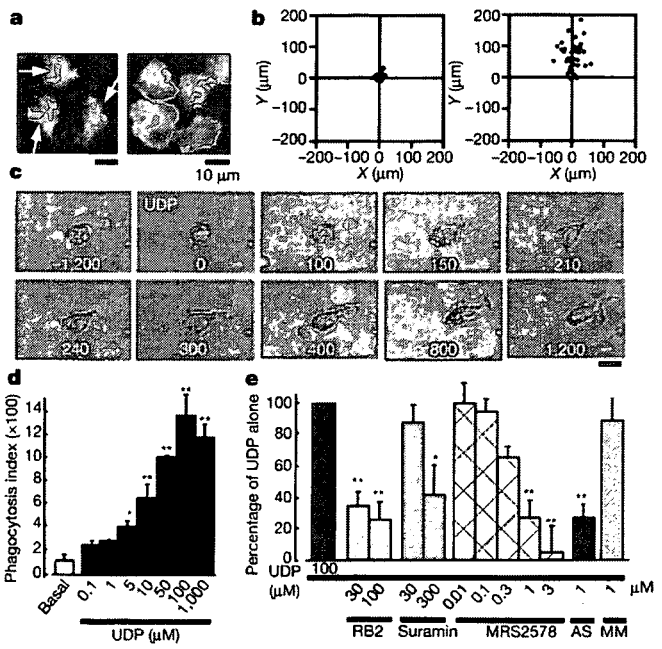

Figure 2 | Changes in cell motilities of microglia. a, UDP- and ATP-evoked membrane ruffles. Cultured microglia were stimulated for 5 min with 100 μM UDP (left) and 10 μM ATP (right), fixed, permeabilized, and then stained with anti-phalloidin. Scale bar, 10 μm. **b**, Typical chemotactic responses of microglia towards 100 μM UDP (left) and 100 μM ATP (right) assessed by the Dunn chemotaxis chamber (see Methods). **c**, Time-lapse images showing the effect of UDP on the microglial morphogenic changes and the uptake of fluorescent zymosan particles (green). The time after addition of UDP is shown in seconds in each picture. **d**, The UDP-evoked uptake of microspheres was assessed quantitatively as a phagocytosis index by using FACS. Data are mean and s.e.m. for three experiments (asterisk, $P < 0.05$; two asterisks, $P < 0.01$ compared with basal). **e**, Effects of the P2 receptor antagonists reactive blue 2 and suramin, the $P2Y_6$ receptor antagonist MRS2578, and $P2Y_6$ AS or MM on the UDP-evoked phagocytosis. Data are means and s.e.m. for three or four experiments (asterisk, $P < 0.05$; two asterisks, $P < 0.01$ compared with UDP alone).

Because phagocytes remove dead or damaged cells, debris and invading pathogens, recognition is the first step in phagocytosis. It is initiated by activation of the phagocytosis-promoting receptors such as Fc receptors and complement receptors[20]. In the central nervous system, microglia possess these receptors and remove amyloid-β, a key molecule in Alzheimer's disease, and attenuate Alzheimer's disease-like pathology[21]. With regard to apoptotic cells, microglia may also remove such cells by recognizing so-called 'eat-me' signals[20]. However, in the present study we used non-opsonized zymosan (Fig. 2c) and latex beads (Fig. 2d, e), which were not recognized by opsonin-dependent receptors such as Fc receptors, complement receptors or vitronectin receptors. Phagocytosis-promoting receptors also include opsonin-independent ones such as β_1-integrins, mannose receptors, scavenger receptors and phosphatidylserine receptors[13]; in fact, microglia expressed all these receptors (Supplementary Fig. 5a–e, cell lysates). Among these receptors, β_1-integrin was detected as a bead-associated protein that was slightly increased on stimulation with UDP (Supplementary Fig. 5a, bead-associated) and localized at membrane ruffle-like or phagocytic cup-like structures (see also Supplementary Fig. 2b), to which fluorescent microspheres were attached (Supplementary Fig. 5f). However, we do not know whether β_1-integrin itself binds or recognizes the microspheres. β_1-Integrin might be involved in some way in the machinery of phagocytosis or in the uptake processes of the microspheres in response to UDP, but the precise target molecule or molecules that bind or recognize microspheres to be phagocytosed remains to be identified. The microglial phagocytosis seen in the present study is a new type that is promoted by the diffusible

extracellular molecule UDP. However, we cannot deny the possibility that the UDP may simply facilitate the machinery of phagocytosis and that UDP-evoked phagocytosis observed in this study may even include macropinocytosis.

To determine the expression and function of microglial $P2Y_6$ receptors *in vivo*, the excitotoxicity of brain injury was induced by kainic acid (KA) (Fig. 3). KA is an excitatory amino acid that is often used to cause limbic motor epilepsy or excitatory neuronal cell death *in vivo* and *in vitro*. KA acts on non-NMDA glutamate receptors to facilitate excess excitability, thereby leading to necrosis and even apoptosis of neurons. The hippocampal CA1 and CA3 regions are susceptible to neuronal death in response to KA[22]. When KA was injected intraperitoneally into rats (10 mg kg^{-1}), it produced typical limbic seizure within 60 min. At 72 h after the administration of KA, the brains were removed and were used for western blotting, immunohistochemical assays and *in situ* hybridization (ISH). Western blotting analysis showed that KA increased the expression of $P2Y_6$ receptors in comparison with the saline-injected control groups (Fig. 3A, B). Double staining of microglia and neurons by anti-Iba1 (green) and anti-neuronal nuclei (NeuN, red) antibodies, respectively, showed that KA induced severe neuronal loss in the hippocampal CA1 and CA3 regions, where intense Iba1-positive signals—indicative of microglia—were observed. KA increased the number of microglia appearing in the activated form with poorly ramified, short and thick processes (Fig. 3C, f–h). Small NeuN signals seemed to be incorporated in some microglia (see g and h in Fig. 3C), suggesting that microglia phagocytose damaged or dead neurons. These findings suggest that microglia might migrate or proliferate, probably as a result of KA-induced neuronal damage.

We further examined the cell types that produced increases in $P2Y_6$ receptor protein in response to the administration of KA, and found that $P2Y_6$ immunoreactivities (green in Fig. 3D) were associated with the microglia (OX-42, red in Fig. 3D, c) but not with astrocytes (glial fibrillary acidic protein (GFAP), red in Fig. 3D, d) or neurons (NeuN, red in Fig. 3D, e). Furthermore, we performed ISH to characterize the expression of mRNA coding for $P2Y_6$ receptors with the use of digoxigenin-labelled antisense RNA probe. Signals for $P2Y_6$ receptor mRNA were very low in the naive animals but were upregulated three days after treatment with KA (Fig. 3E, b; blue dots indicated by arrowheads). At this time, the number of microglia increased markedly, especially at the hippocampal CA3 and CA1 regions (Fig. 3C). After ISH, the sections were stained with anti-Iba1 antibody to characterize $P2Y_6$ receptor mRNA signals. In the hippocampal CA3 regions of naive rats, there were very few anti-Iba1-positive microglia that did not show $P2Y_6$ receptor mRNA. In contrast, in the hippocampal CA3 of KA-injected rats, there was an increased number of anti-Iba1-positive microglia, in which $P2Y_6$ receptor signals were colocalized with microglia (Fig. 3E, c; KA, black arrows, see also inset at higher magnification).

There is a growing literature about 'eat-me' signals that are expressed on the cell surface of apoptotic or dying cells. However, diffusible signals that trigger phagocytosis have received only limited attention. When neurons or cells are exposed to traumatic injury such as ischaemia, they swell and subsequently shrink as a result of

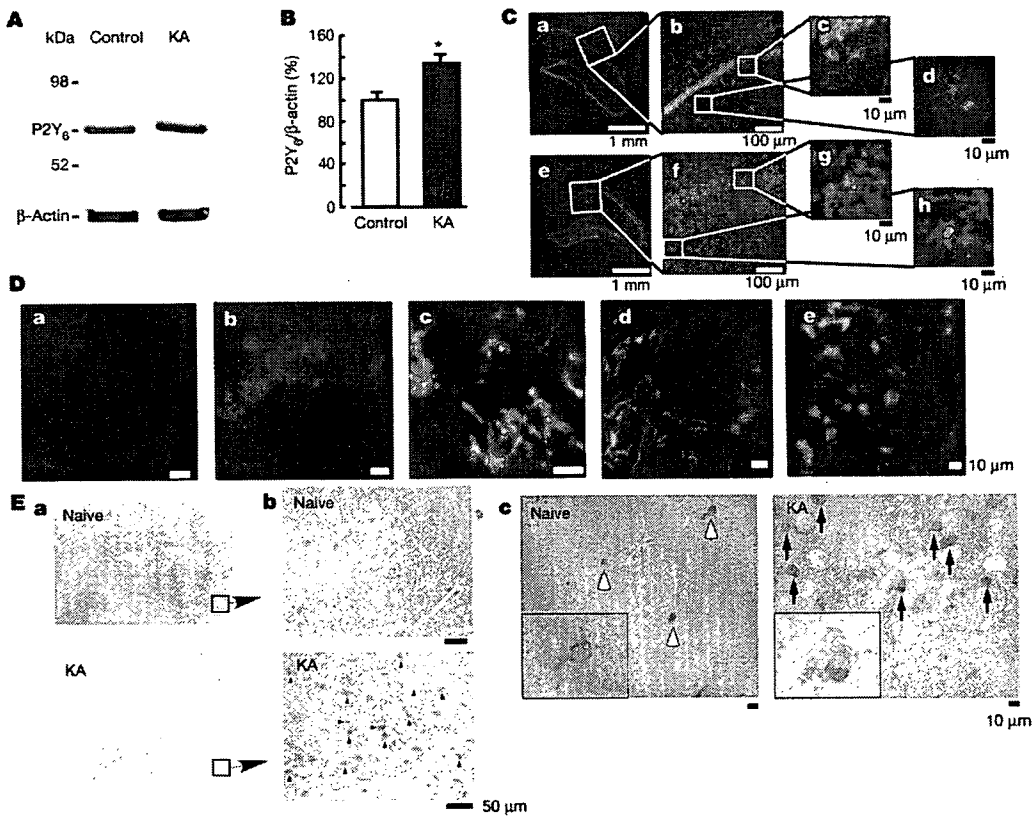

Figure 3 | Increase in $P2Y_6$ receptors in the hippocampus after kainic acid (KA)-treatment. A, Western blot analysis, showing increase in $P2Y_6$ receptor protein in rats treated intraperitoneally with 10 mg kg^{-1} KA, 72 h after treatment. **B**, Summary of quantitative data; KA was applied at 10 mg kg^{-1}. Results are means and s.e.m. for 8 (control) and 7 (KA) experiments (asterisk, $P < 0.05$ compared with control). **C**, Immunohistochemical analysis in naive control (**a–d**) and KA-treated (**e–h**) rats; red, anti-NeuN antibody; green, anti-Iba1 antibody. Rectangles in **a** and **e** are expanded in **b** and **f**, respectively. Rectangles in **b** and **f** also correspond to **c**, **d** and **g**, **h**, respectively. **D**, Anti-$P2Y_6$ antibody signals (green) were increased by KA (**a**, control; **b**, KA), which was colocalized with microglia (red in **c**, anti-OX42) but not with astrocytes (red in **d**, anti-GFAP) or neurons (red in **e**, anti-NeuN). **E**, ISH analysis. **a**, **b**, mRNA coding for $P2Y_6$ receptor in naive rats was very low but was increased at the hippocampal CA3 region by KA (3 days later) (blue dots and arrowheads, KA). **c**, Double staining with $P2Y_6$ antisense RNA probe (blue dots) and anti-Iba-1 antibody (brown signals, white (naive) or black (KA) arrows). In KA-treated rats there was an increased number of microglia, which was associated with $P2Y_6$ receptor mRNA (blue signals, inset at higher magnification in KA).

increased permeability. This is followed by leakage of cytoplasmic molecules, leading to necrotic cell death. Thus, cytoplasmic nucleotides could be diffusible messengers that signal the crisis state to adjacent cells including microglia. In fact, the diffusible messenger ATP promotes microglial chemotaxis and/or migration[3–6]. Diffusible molecules might be insufficiently precise to cause phagocytes to recognize and eat cells. However, released or leaked nucleotides are immediately degraded by the extracellular nucleotide-degrading enzymes. In this respect, UDP might be a localized and transient marker of traumatized or necrotic cells.

Cell injury results in a leakage of ATP that affects the motility of adjacent cells, including microglia[3,4]. In addition, cells release or leak uridine nucleotides[23] and nucleotide sugars[24] in response to various stimuli or ischaemic injury[25]. We therefore next investigated whether KA increases the release of extracellular UDP from neurons to induce microglial phagocytosis. Cultured hippocampal neurons were stimulated with and without 100 μM KA for 1 h; the supernatant was then collected for nucleotide assay by high-performance liquid chromatography (HPLC) or for phagocytosis assay by FACS (Fig. 4). Because released or leaked UTP is rapidly degraded into UDP, UMP and uridine by ARL67156-sensitive ectonucleotidases, we monitored the amount of UTP rather than UDP, and collected the supernatant and the microdialysates in the presence of 20 μM ARL67156 throughout experiments. There was a close relationship between the HPLC peak corresponding to UTP and the concentration of the standard UTP ($R^2 = 0.9947$). The amount of UTP in the KA-treated supernatant was significantly larger than that in the KA-untreated control supernatant (Fig. 4b; control, 2.3 ± 1.1 μM; KA treated, 10.5 ± 3.9 μM, $P < 0.05$). We also tested whether the KA-treated supernatant obtained from cultured hippocampal neurons facilitated microglial phagocytosis. Hippocampal neurons were treated with and without 100 μM KA for 1 h; each supernatant was collected and added to microglia; this was followed by a phagocytosis assay. As shown in Fig. 4c, when microglia were incubated with the KA-treated supernatant for 20 min, there was a significant increase in phagocytosis, which was blocked by the $P2Y_6$ receptor antagonist MRS2578 (1 μM). KA alone did not stimulate phagocytosis.

Finally, we tested whether KA induces the release of UDP and $P2Y_6$-receptor-mediated phagocytosis *in vivo*. An increase in extracellular UTP concentration ($[UTP]_o$) was observed soon after injection of KA (from 1 to 4 h after injection), which reached 2–3-fold higher than the KA-untreated control (data not shown). At 1 day after KA injection, $[UTP]_o$ was about 1.5–2.0-fold higher than the KA-untreated control (Fig. 4e). Then, at day 3, $[UTP]_o$ reached almost 10-fold higher levels (9.4 ± 1.2-fold; Fig. 4e and inset), which decreased slightly at day 5. A higher (5–10-fold) $[UTP]_o$ was observed 2–3 days after the injection of KA, which lasted at least another couple of days. It should be noted that loss of neurons (removal of neurons) also became obvious 2–3 days after the KA injection. We further injected fluorescent microspheres into the hippocampal CA3 regions of KA-treated rats, and then counted the numbers of the microspheres phagocytosed or attached by microglia. The $P2Y_6$ receptor antagonist MRS2578 was injected into the hippocampal CA3 region, and $P2Y_6$ AS or MM (mismatch oligonucleotide) was injected into the third ventricle. The number of microspheres taken or attached by microglia was markedly increased by KA treatment, which is significantly inhibited by MRS2578 or $P2Y_6$ AS but not by MM (Fig. 4g; see also Supplementary Fig. 6). These findings all suggest that UDP/$P2Y_6$-receptor-mediated signals are important for microglial phagocytosis even *in vivo*.

A recent review described that dying cells use both 'find-me' and 'eat-me' signals for phagocyte attraction and recognition[26]. Nucleotides could be both 'find-me' and 'eat-me' signals. The intracellular ATP concentration is estimated to be high (more than 5 mM) and the UTP concentration is reported to be one-third that of ATP[23]. Cells release ATP, and here we showed that KA caused an increase in extracellular UTP or UDP. Microglia might therefore be attracted by ATP or ADP[5,6] and subsequently recognize UDP, leading to the removal of the dying cells or their debris. It is interesting that ATP/ADP is not able to efficiently activate $P2Y_6$ receptors; neither can UDP act on $P2Y_{12/13}$ receptors. Thus, even if these nucleotides were leaked or released simultaneously, adenine and uridine nucleotides would regulate microglial motilities, namely chemotaxis and phagocytosis, in a mutually exclusive but coordinated fashion.

So far we have not shown quantitative data indicating that individual microglia upregulate the expression of $P2Y_6$ receptors. A significant, but not drastic, increase in $P2Y_6$ receptor protein in the hippocampus was observed after injection of KA (Fig. 3A, B). ISH data show that expression of mRNA coding for $P2Y_6$ receptors in microglia was very low in naive animals but became obvious in an increased number of microglia after KA injection (Fig. 3E), suggesting that the increase in $P2Y_6$ receptor protein is not due simply to an increased number of microglia but is upregulated in individual

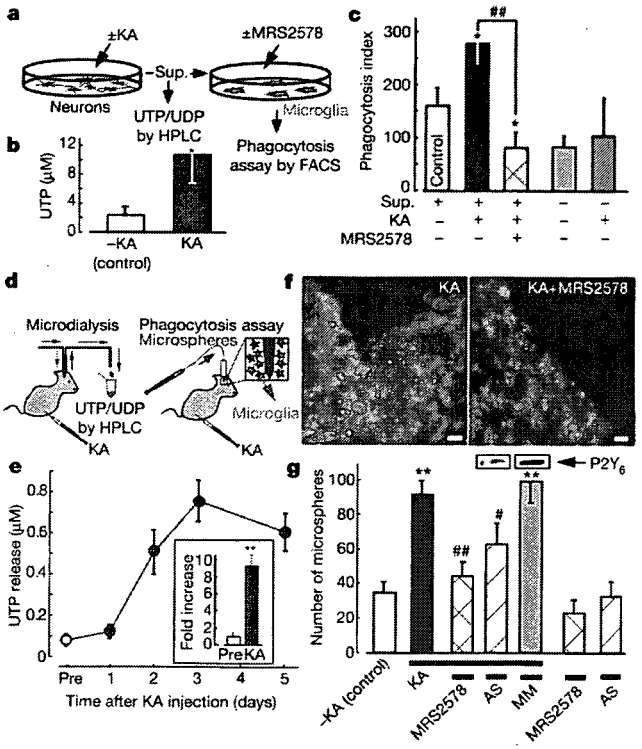

Figure 4 | KA-evoked increases in extracellular uridine nucleotides and $P2Y_6$-receptor-mediated microglial phagocytosis *in vitro* and *in vivo*. **a**, Schematic diagram of the experiments *in vitro*. Sup., supernatant. **b**, Summary of the UTP concentration in the KA-treated and control supernatants. Data show means and s.e.m. for at least five independent experiments (asterisk, $P < 0.05$ compared with control). **c**, Effects of the KA-treated and control supernatant on microglial uptake of fluorescent latex beads. Data show means and s.e.m. for at least four independent experiments (asterisk, $P < 0.05$ compared with control; hash sign, $P < 0.05$ compared with KA-treated supernatant). **d**, Schematic diagram of the experiments *in vivo*. KA was applied intraperitoneally at 10 mg kg^{-1}. **e**, Time course of changes in $[UTP]_o$ in baseline dialysates (before treatment with KA (Pre), and 1, 2, 3 and 5 days afterwards). Inset, fold increase at day 3 (compared with before treatment). **f**, Typical pictures of fluorescent microspheres (green) attached or taken up by microglia (red, anti-Iba1) in the KA-treated (left) and KA + MRS2578-treated (right) hippocampal CA3 regions. Scale bar, 20 μm. **g**, Quantitative analysis of phagocytosis *in vivo* (details are provided in Supplementary Methods). Changes in $P2Y_6$ receptor protein by $P2Y_6$ AS or MM are shown at the top of corresponding columns. Values are means and s.e.m. (asterisk, $P < 0.01$ compared with control (−KA); hash sign, $P < 0.05$; two hash signs, $P < 0.01$ compared with KA-treated group). Statistical analyses were performed by ANOVA with Scheffe's multiple comparison. At least three sections containing the injection sites were analysed per animal, and at least three animals were used in each group for analysis.

microglia. We also emphasize that even if the extent of $P2Y_6$ receptor upregulation is not drastic, an increase in extracellular UDP, a ligand for $P2Y_6$ receptor, is markedly increased after treatment with KA (detected as UTP, almost 10-fold; Fig. 4e) and therefore that the UDP/$P2Y_6$ receptor system would be sufficiently activated to cause microglial phagocytosis after treatment with KA. In comparison with the extensive knowledge of the molecular events involved in the regulation of apoptosis or necrosis, relatively little is known about the processes responsible for the clearance of dead cells and the degradation of waste materials. Considering the present findings that injured neurons leak diffusible UTP/UDP and cause the upregulation of $P2Y_6$ receptors in microglia, the UDP/$P2Y_6$ receptor system might function as a critical device covering the phagocytosis of both apoptotic and necrotic cells if they release or leak UDP by sensing diffusible UDP signals.

Thus we have shown that microglia express $P2Y_6$ receptors that function as a sensor of phagocytosis. The $P2Y_6$ receptor agonist UDP is released (as UTP) when neurons are damaged by KA. Thus, the activation of $P2Y_6$ receptors by UDP would be a key event in initiating the clearance of dying cells or debris in the central nervous system.

METHODS

Detailed methods are provided in Supplementary Information.

Microglia culture. The protocol was reviewed and approved by the Committee for Institutional Laboratory Animal Care of the National Institute of Health Sciences. Rat primary cultured microglia were prepared in accordance with the method described previously[27].

Phagocytosis assay *in vitro* and *in vivo*. *In vitro* microglial phagocytosis was assessed by either FACScan analysis or imaging analysis with fluorescently labelled microspheres. For the *in vivo* phagocytosis assay, fluorescently labelled microspheres were injected into the hippocampal CA3 region after injection of KA, and then the number of fluorescent microspheres associated with microglia was analysed by confocal microscopy (LSM 5 Pascal; Carl Zeiss).

Microdialysis. A microdialysis probe (A-I type probe; Eicom) was inserted into the hippocampal CA3 region by means of a guide cannula, and was perfused continuously at a flow rate of 3.0 $\mu l\ min^{-1}$ (collected for 60 min) supplemented with the ectonuclease inhibitor ARL67156 (20 μM) (Sigma).

Quantification of UTP by HPLC. The concentration of nucleotides in the supernatant of the hippocampal cultures was analysed with an HPLC system (Jasco) combined with a C_{18} column (4.6 × 250 mm, Shodex) as described[28], with minor modifications.

Data analysis and statistics. All results are expressed as means ± s.e.m. A statistical analysis was performed with Student's *t*-test or analysis of variance, followed by Scheffe's multiple comparison test. Differences were considered to be significant at $P < 0.05$.

Received 23 December 2006; accepted 23 February 2007.
Published online 4 April 2007.

1. Guthrie, P. B. *et al.* ATP released from astrocytes mediates glial calcium waves. *J. Neurosci.* **19**, 520–528 (1999).
2. Koizumi, S., Fujishita, K., Tsuda, M., Shigemoto-Mogami, Y. & Inoue, K. Dynamic inhibition of excitatory synaptic transmission by astrocyte-derived ATP in hippocampal cultures. *Proc. Natl Acad. Sci. USA* **100**, 11023–11028 (2003).
3. Nimmerjahn, A., Kirchhoff, F. & Helmchen, F. Resting microglial cells are highly dynamic surveillants of brain parenchyma *in vivo*. *Science* **308**, 1314–1318 (2005).
4. Davalos, D. *et al.* ATP mediates rapid microglial response to local brain injury *in vivo*. *Nature Neurosci.* **8**, 752–758 (2005).
5. Honda, S. *et al.* Extracellular ATP or ADP induce chemotaxis of cultured microglia through $G_{i/o}$-coupled P2Y receptors. *J. Neurosci.* **21**, 1975–1982 (2001).
6. Nasu-Tada, K., Koizumi, S. & Inoue, K. Involvement of β1 integrin in microglial chemotaxis and proliferation on fibronectin: different regulations by ADP through PKA. *Glia* **52**, 98–107 (2005).
7. Ferrari, D. *et al.* P2Z purinoreceptor ligation induces activation of caspases with distinct roles in apoptotic and necrotic alterations of cell death. *FEBS Lett.* **447**, 71–75 (1999).
8. Suzuki, T. *et al.* Production and release of neuroprotective tumor necrosis factor by P2X7 receptor-activated microglia. *J. Neurosci.* **24**, 1–7 (2004).
9. Tsuda, M. *et al.* P2X4 receptors induced in spinal microglia gate tactile allodynia after nerve injury. *Nature* **424**, 778–783 (2003).
10. Chang, K., Hanaoka, K., Kumada, M. & Takuwa, Y. Molecular cloning and functional analysis of a novel P2 nucleotide receptor. *J. Biol. Chem.* **270**, 26152–26158 (1995).
11. Communi, D., Parmentier, M. & Boeynaems, J. M. Cloning, functional expression and tissue distribution of the human P2Y6 receptor. *Biochem. Biophys. Res. Commun.* **222**, 303–308 (1996).
12. Mamedova, L. K., Joshi, B. V., Gao, Z. G., von Kugelgen, I. & Jacobson, K. A. Diisothiocyanate derivatives as potent, insurmountable antagonists of P2Y6 nucleotide receptors. *Biochem. Pharmacol.* **67**, 1763–1770 (2004).
13. Greenberg, S. Signal transduction of phagocytosis. *Trends Cell Biol.* **5**, 93–99 (1995).
14. Mitchison, T. J. & Cramer, L. P. Actin-based cell motility and cell locomotion. *Cell* **84**, 371–379 (1996).
15. Lauffenburger, D. A. & Horwitz, A. F. Cell migration: a physically integrated molecular process. *Cell* **84**, 359–369 (1996).
16. Ohsawa, K., Imai, Y., Kanazawa, H., Sasaki, Y. & Kohsaka, S. Involvement of Iba1 in membrane ruffling and phagocytosis of macrophages/microglia. *J. Cell Sci.* **113**, 3073–3084 (2000).
17. Kreutzberg, G. W. Microglia: a sensor for pathological events in the CNS. *Trends Neurosci.* **19**, 312–318 (1996).
18. Nicholas, R. A. *et al.* Pharmacological and second messenger signalling selectivities of cloned P2Y receptors. *J. Auton. Pharmacol.* **16**, 319–323 (1996).
19. Mellor, E. A., Maekawa, A., Austen, K. F. & Boyce, J. A. Cysteinyl leukotriene receptor 1 is also a pyrimidinergic receptor and is expressed by human mast cells. *Proc. Natl Acad. Sci. USA* **98**, 7964–7969 (2001).
20. Lauber, K. *et al.* Apoptotic cells induce migration of phagocytes via caspase-3-mediated release of a lipid attraction signal. *Cell* **113**, 717–730 (2003).
21. Bard, F. *et al.* Peripherally administered antibodies against amyloid β-peptide enter the central nervous system and reduce pathology in a mouse model of Alzheimer disease. *Nature Med.* **6**, 916–919 (2000).
22. Sperk, G. *et al.* Kainic acid induced seizures: neurochemical and histopathological changes. *Neuroscience* **10**, 1301–1315 (1983).
23. Lazarowski, E. R., Homolya, L., Boucher, R. C. & Harden, T. K. Direct demonstration of mechanically induced release of cellular UTP and its implication for uridine nucleotide receptor activation. *J. Biol. Chem.* **272**, 24348–24354 (1997).
24. Lazarowski, E. R., Shea, D. A., Boucher, R. C. & Harden, T. K. Release of cellular UDP-glucose as a potential extracellular signaling molecule. *Mol. Pharmacol.* **63**, 1190–1197 (2003).
25. Erlinge, D. *et al.* Uridine triphosphate (UTP) is released during cardiac ischemia. *Int. J. Cardiol.* **100**, 427–433 (2005).
26. Ravichandran, K. S. 'Recruitment signals' from apoptotic cells: invitation to a quiet meal. *Cell* **113**, 817–820 (2003).
27. Nakajima, K. *et al.* Identification of elastase as a secretory protease from cultured rat microglia. *J. Neurochem.* **58**, 1401–1408 (1992).
28. Lazarowski, E. R., Boucher, R. C. & Harden, T. K. Constitutive release of ATP and evidence for major contribution of ecto-nucleotide pyrophosphatase and nucleoside diphosphokinase to extracellular nucleotide concentrations. *J. Biol. Chem.* **275**, 31061–31068 (2000).

Supplementary Information is linked to the online version of the paper at www.nature.com/nature.

Acknowledgements We thank T. Shimizu and Dr. S. Ishii for providing CysLT1 receptor-expressed Chinese hamster ovary cells; K. Sakemi for technical assistance; Y. Sasaki for helpful suggestions; K. Suzuki and R. Adachi for allowing us to use the Pascal confocal microscope system; and T. Nishimaki-Mogami, Y. Ohno and T. Nagao for continuous encouragement. This study was supported in part by a grant from The National Institute of Biomedical Innovation, a grant from Uehara Memorial Foundation, a Grant-in-Aid for Scientific Research on Priority Areas, for Creative Scientific Research, Scientific Research (A and B), and for Young Scientists (A) from the Ministry of Education, Science, Sports and Culture of Japan.

Author Contributions S.K. designed most experiments, performed Ca^{2+} imaging and *in vivo* experiments and wrote the paper. Y.S.M. conducted major parts of the experiments. K.N.T. and Y.S. carried out the FACS assay and the HPLC analysis, respectively. K.O. and S.K. performed the chemotaxis analysis. B.V.J. and K.A.J. made the $P2Y_6$ receptor antagonist MRS2578. M.T. analysed the data. K.I. analysed the data and coordinated the project. K.I. also designed the project. All authors discussed the results and commented on the manuscript.

Author Information Reprints and permissions information is available at www.nature.com/reprints. The authors declare no competing financial interests. Correspondence and requests for materials should be addressed to K.I. (inoue@phar.kyushu-u.ac.jp).

GLIA 55:604–616 (2007)

Involvement of $P2X_4$ and $P2Y_{12}$ Receptors in ATP-Induced Microglial Chemotaxis

KEIKO OHSAWA,[1] YASUHIRO IRINO,[1] YASUKO NAKAMURA,[1] CHIHIRO AKAZAWA,[1] KAZUHIDE INOUE,[2] AND SHINICHI KOHSAKA[1]*

[1]*Department of Neurochemistry, National Institute of Neuroscience, Kodaira, Tokyo 187-8502, Japan*

[2]*Department of Pharmacology, Graduate School of Pharmaceutical Sciences, Kyushu University, Higashi, Fukuoka 812-8582, Japan*

KEY WORDS

microglia; ATP; chemotaxis; P2Y12; P2X4

ABSTRACT

We previously reported that extracellular ATP induces membrane ruffling and chemotaxis of microglia and suggested that their induction is mediated by the Gi/o-protein coupled $P2Y_{12}$ receptor ($P2Y_{12}R$). Here we report discovering that the $P2X_4$ receptor ($P2X_4R$) is also involved in ATP-induced microglial chemotaxis. To understand the intracellular signaling pathway downstream of $P2Y_{12}R$ that underlies microglial chemotaxis, we examined the effect of two phosphatidylinositol 3′-kinase (PI3K) inhibitors, wortmannin, and LY294002, on chemotaxis in a Dunn chemotaxis chamber. The PI3K inhibitors significantly suppressed chemotaxis without affecting ATP-induced membrane ruffling. ATP stimulation increased Akt phosphorylation in the microglia, and the increase was reduced by the PI3K inhibitors and a $P2Y_{12}R$ antagonist. These results indicate that $P2Y_{12}R$-mediated activation of the PI3K pathway is required for microglial chemotaxis in response to ATP. We also found that the Akt phosphorylation was reduced when extracellular calcium was chelated, suggesting that ionotropic P2X receptors are involved in microglial chemotaxis by affecting the PI3K pathway. We therefore tested the effect of various $P2X_4R$ antagonists on the chemotaxis, and the results showed that pharmacological blockade of $P2X_4R$ significantly inhibited it. Knockdown of the $P2X_4$ receptor in microglia by RNA interference through the lentivirus vector system also suppressed the microglial chemotaxis. These results indicate that $P2X_4R$ as well as $P2Y_{12}R$ is involved in ATP-induced microglial chemotaxis.

INTRODUCTION

Microglia are the immune effector cells that participate in tissue repair, amplification of inflammatory responses, and neuronal degeneration in the central nervous system (CNS) (Kreutzberg, 1996; Streit, 2002). They are present in the form of ramified cells under normal conditions, but in response to pathological stimuli microglia rapidly transform into a motile ameboid form and migrate toward lesion sites, where they secrete a variety of substances and clear cell debris (Moran and Graeber, 2004; Nakajima and Kohsaka, 2005; Stence et al., 2001). Thus, microglial migration plays a crucial role in the amelioration of a damaged CNS; however, the intracellular signals underlying microglial cell migration are poorly understood.

Extracellular ATP is known to play a role as a neurotransmitter or neuromodulator in the CNS (Illes and Alexandre Ribeiro, 2004), and it regulates various physiological functions of microglia (Inoue, 2002). ATP receptors are classified into two families: the ionotropic P2X receptor (P2XR) family and the GTP-binding (G-) protein coupled P2Y receptor (P2YR) family (Ralevic and Burnstock, 1998), and microglia have been reported to possess functional ATP receptors, including $P2X_4R$, $P2X_7R$, and $P2Y_{12}R$ (Cavaliere et al., 2003; James and Butt, 2002; Sasaki et al., 2003; Tsuda et al., 2003). Davalos et al. (2005) and Nimmerjahn et al. (2005) recently reported that processes of ramified microglia extended toward a confocal laser injury, where ATP is likely to be released by damaged tissue and surrounding astrocytes. These observations suggest that ATP is a primary molecule in the induction of the change in microglial morphology.

We have also previously reported that ATP-induced microglial membrane ruffling and chemotaxis are mediated by Gi/o-protein coupled $P2Y_{12}R$ (Honda et al., 2001; Sasaki et al., 2003); however, the intracellular signaling pathway downstream of $P2Y_{12}R$ following ATP stimulation is not fully understood. Several recent articles have revealed that $P2Y_{12}R$ stimulation results in activation of the phosphatidylinositol 3′-kinase (PI3K) pathway in some cells (Czajkowski et al., 2004; Soulet et al., 2004; Van Kolen and Slegers, 2004). Although PI3K is known to be a crucial enzyme in the regulation of chemotaxis by monocytes and macrophages (Procko and McColl, 2005; Ridley, 2001; Van Haastert and Devreotes, 2004), whether the PI3K pathway participates in ATP-induced microglial chemotaxis remained unclear.

This article contains supplementary material available via the Internet at http://www.interscience.wiley.com/jpages/0894-1491/suppmat

Grant sponsors: Japanese Ministry of Health, Labour, and Welfare; Japanese Ministry of Education, Culture, Sports, Science, and Technology.

*Correspondence to: Shinichi Kohsaka, Department of Neurochemistry, National Institute of Neuroscience, 4-1-1 Ogawahigashi, Kodaira, Tokyo 187-8502, Japan. E-mail: kohsaka@ncnp.go.jp

Received 7 August 2006; Accepted 26 December 2006

DOI 10.1002/glia.20489

Published online 13 February 2007 in Wiley InterScience (www.interscience.wiley.com).

In this study we demonstrated that activation of the PI3K pathway is required for ATP-induced microglial chemotaxis and found that the PI3K/Akt activation was suppressed when extracellular Ca^{2+} was chelated. ATP stimulates P2XRs in microglia and causes an increase in intracellular calcium concentration ($[Ca^{2+}]_i$) by inducing an extracellular Ca^{2+} influx (Inoue et al., 1998; Tsuda et al., 2003). Therefore, to clarify involvement of P2XRs in microglial chemotaxis we also examined the effect of antagonists and RNA interference (RNAi) with P2XRs on microglial chemotaxis, and the results demonstrated that P2X$_4$R is involved in ATP-induced chemotaxis.

MATERIALS AND METHODS

Isolation of Microglia

Microglia were obtained from primary cell cultures of neonatal Wistar rat cerebral cortex as described previously (Nakajima et al., 1992). In brief, mixed glial cultures were maintained for 12–23 days in DMEM (Invitrogen, Carlsbad, CA) with 10% fetal calf serum (FCS) (Irvine Scientific, Santa Ana, CA). Microglia were prepared as floating cells by gentle shaking and allowed to attach to appropriate dishes or glasses.

Membrane Ruffling

Microglia attached to glass coverslips were incubated for 4 h in DMEM without FCS and stimulated with 50 μM ATP (Yamasashyoyu, Chiba, Japan) for 5 min at 37°C. The cells were then fixed with 3.7% formaldehyde for 10 min, permeabilized for 5 min with PBS containing 0.1% Triton X-100, and stained for 1 h with 2 U/mL Texas Red-conjugated phalloidin (Invitrogen) diluted in PBS containing 1%BSA. The cells were mounted in PermaFluor (Thermo Fisher Scientific, Waltham, MA) and examined under a fluorescence microscope AX70 (Olympus, Tokyo, Japan). To quantify membrane ruffles, cells were stained with 1 μg/mL anti-Iba1 polyclonal antibody (Imai et al., 1996) and Alexa Fluor 488-conjugated anti-rabbit IgG (1:1,000, Invitrogen) and then incubated with 2 U/mL Alexa Fluor 647-conjugated phalloidin (Invitrogen). The F-actin content of cells positive for Iba1 was quantified as the integral intensity of Alexa Fluor 647 fluorescence with a laser scanning cytometer (LSC2, CompuCyte, Cambridge, MA). The mean fluorescent intensity of the cells pretreated with each inhibitor was calculated from the data obtained from 1,000 cells. Increases in membrane ruffles are reported as ratios of the mean fluorescent intensity of the ATP-stimulated cells to that of the unstimulated cells. The effect of the inhibitors was assessed by preincubating cells with wortmannin (Sigma, St. Louis, MO) (100 nM) for 20 min, LY294002 (Wako, Osaka Japan) (50 μM) for 20 min, AR-C69931MX (AstraZeneca, UK) (1 μM) for 10 min, 2′,3′-*O*-(2,4,6-trinitrophenyl) adenosine 5-triphosphate (TNP-ATP) (Invitrogen) (100 μM) for 5 min, pyridoxal-phosphate-6-azophenyl-2′,4′-disulfonic acid (PPADS) (Sigma) (300 μM) for 5 min, or Brilliant blue G (BBG) (Nacalai Tesque, Kyoto, Japan) (1 μM) for 5 min, and then stimulating them with ATP.

Chemotaxis Assay

Dunn chemotaxis chambers (Weber Scientific International, Teddington, UK) were used to perform the chemotaxis assays according to the method described previously (Honda et al., 2001; Webb et al., 1996). In brief, microglia attached to square coverslips were incubated for 4 h in DMEM without FCS. Each coverslip was then inverted onto a chamber and the medium in the outer well was replaced with DMEM containing 50 μM ATP. The chamber was placed on the stage of a microscope (ECLIPSE TE300; Nikon, Tokyo Japan), and cell images were collected every 5 min for 1 h with a CCD camera (Hamamatsu Photonics, Hamamatsu, Japan) and imaging software (fishPPC; Hamamatsu Photonics). Time-lapse video images were used to calculate the final position of cells relative to their starting position, and the distance each cell migrated was measured by plotting the positions of the cell nucleus on a computer display with software (Image-Pro Plus; Media Cybernetics, MD). The distance and direction moved are shown as x and y coordinates on scatter diagrams in which the x-axis is parallel to the outer ring and the position of the outer well is above the y-axis.

Akt Activation

Microglia were incubated for 4 h in DMEM without FCS and then stimulated with 50 μM ATP or 100 ng/mL recombinant murine macrophage-colony stimulating factor (M-CSF) (R&D Systems, Minneapolis, MN) for 5 min at 37°C, and lysed with SDS sample buffer. Proteins were separated by 10% SDS-PAGE and transferred onto an Immobilon P membrane (Millipore, MA). The membrane was incubated for 1 h at room temperature with a blocking solution containing 25 mM Tris, pH 7.5, 150 mM NaCl, 0.1%(v/v) Tween 20 (TTBS), and 5% (v/v) nonfat dry milk, and then incubated overnight at 4°C with mouse monoclonal anti-phospho-Akt (Ser473) antibody (diluted 1:1,000, Cell Signaling Technology, Beverly, MA) or rabbit polyclonal Akt antibody (diluted 1:1,000, Cell Signaling Technology). The membrane was incubated for 1 h at room temperature with horseradish peroxidase (HRP)-conjugated donkey anti-mouse IgG (diluted 1:1,000, GE Healthcare, Little Chalfont, UK) or HRP-conjugated donkey anti-rabbit IgG (diluted 1:1,000, GE Healthcare), and phosphorylated Akt and total Akt were detected with an ECL Western blotting detection system (GE Healthcare). The Akt phosphorylation level was quantified by densitometry with NIH image software. Before stimulating the cells in the calcium-depleted experiment, they were incubated for 30 min in a balanced salt solution composed of 20 mM Hepes, pH7.4, 150 mM NaCl, 5 mM KCl, 1.2 mM $MgCl_2$, and 10 mM glucose in the presence of 1.2 mM Ca^{2+} (BSS) or 1 mM ethy-

lene glycol-*bis*(2-aminoethyl)-*N,N,N,N*-tetraacetic acid (EGTA) (Ca^{2+}-free BSS).

Construction of Lentivirus Vectors Expressing Interfering Short Hairpin RNA (shRNAi) and Microglial Transduction

Lentivirus containing shRNAi was prepared by the method previously described (Yogosawa et al., 2005). The self-inactivating (SIN) vector construct pCS-RfA-CG, which contains the EGFP gene under the control of the CMV promoter and sites for site-specific recombination with a Gateway vector (attR1,2), was used for simultaneous expression of EGFP and shRNA. Plasmid containing $P2X_4R$ shRNAi under the control of human U6 promoter was provided by Dr. K. Inoue (Kyushu Univ. Fukuoka, Japan). The gene of the $P2X_4R$ shRNAi-expressing cassette inserted into pENTR™1A was transferred into the pCS-RfA-CG by a recombination reaction using Gateway LR Clonase (Invitrogen). The sequence of shRNA targeted for firefly luciferase was used as a control (Nishitsuji et al., 2004). The sequence was inserted into the piGENE™ hU6 *Bsp*MI vector (iGENE Therapeutics, Tsukuba, Japan), and the gene of the luciferase shRNAi-expressing cassette was ligated into the pCS-RfA-CG. The sequence of $shP2X_4R$ was: 5′-GGG ATA AGA GAT ATA GGT AAC GTG TGC TGT CCG TTA CTT ATA TTT CTT GTC CCT TTT T-3′. We confirmed the specificity of P2×4R shRNAi by a coexpression assay. pCS-shP2×4R-CG was cotransfected into Cos7 cells with P2×4 expression plasmid (provided by Dr. K. Inoue) or HA-tagged P2Y12R plasmid (Supplemental information). pCS-shP2×4R-CG significantly suppressed P2×4R expression but had no effect P2Y12R expression. The recombined plasmid was cotransfected into 293FT cells (Invitrogen) with a packaging plasmid (pCAG-HIVgp) and a plasmid expressing Rev and vesicular stomatitis virus G glycoprotein (pCMV-VSV-G-RSV-Rev), and the supernatant was collected after 48 h and filtered through a 0.45-μm pore filter (Falcon). Viral particles in the supernatant were concentrated by ultracentrifugation for 2 h at 19,400 rpm (SW28 rotor; Beckmann Coulter, CA) and recovered by suspension in Hanks buffered saline (Invitrogen).

The recombinant lentivirus (2×10^5 infectious units) was added to the mixed glial cells that had been cultured for 12 days in a 25-cm^2 flask, and cultured for 6 days in DMEM containing 10% FCS. Floating cells were collected as microglia and allowed to attach to appropriate dishes or glasses. The efficiency of microglia transduction with the $shP2X_4R$ vector was 20–30%, the same as with the shControl vector according to an analysis of the number of microglia expressing EGFP by flow cytometry.

Isolation of EGFP-Positive Microglia

After transduction with the lentivirus vectors, floating cells collected as microglia were resuspended in PBS containing 2% FCS. EGFP-positive and -negative cells were sorted with a FACSVantageSE flow cytometry system (BD Biosciences). Live gating was performed with propidium iodide (Sigma-Aldrich, St. Louis, MO). The purity of the EGFP-positive cells was >99% according to a flow cytometry analysis.

Western Blot Analysis of P2X Receptor Expression

Sorted cells were lysed in SDS sample buffer. $P2X_4R$, $P2X_7R$, EGFP, and actin proteins in the lysate equivalent to 2×10^4 cells were separated by 10% SDS-PAGE and detected by Western blot analysis with 1 μg/mL anti-$P2X_4R$ antibody (Alomone Labs, Jerusalem, Israel), 0.6 μg/mL anti-$P2X_7R$ (Alomone Labs), anti-GFP antibody (diluted 1:1,000, Medical & Biological Laboratories, Nagoya, Japan), and anti-actin antibody (diluted 1:1,000, Sigma), respectively, and visualized with the ECL system.

RT-PCR Analysis for $P2Y_{12}R$ Gene Transcripts

RNA was isolated from the sorted cells with the RNeasy Mini Kit (QIAGEN, Hildem, Germany) containing a DNase treatment, according to the manufacturer's protocols. Reverse transcription of RNA was performed with SuperScript III reverse transcriptase (Invitrogen). The PCR amplification conditions were 30 s at 94°C, 15 s at 60°C, and 30 s at 68°C for 25–35 cycles, except for the initial denaturation step of 2 min at 94°C and the final cycle with an elongation step of 5 min at 68°C. An extra reaction mixture without reverse transcriptase was used as a control for DNA contamination of the RNA sample. The primers used were as follows: rat $P2Y_{12}R$, 5′-AAA CTT CCA GCC CCA GCA ATC T-3′ (forward), 5′-CAA GGC AGG CGT TCA AGG AC-3′ (reverse); rat β-actin, as an internal standard, 5′-TTG TTA CCA ACT GGG ACG ACA TGG-3′ (forward), 5′-GAT CTT GAT CTT CAT GGT GCT AGG-3′ (reverse). PCR products of 447 bp for $P2Y_{12}R$ and 763 bp for β-actin were analyzed on a 1.5% agarose and stained with ethidium bromide. The relative intensity of the bands for $P2Y_{12}R$ was quantified by densitometry with NIH image software and normalized to the β-actin products. The normalized values were used to calculate the ratio of $P2Y_{12}R$ mRNA level in the EGFP-positive cells transduced with the $shP2X_4R$ vector to the level in the EGFP-positive cells transduced with the shControl vector.

Calcium Imaging

The intracellular calcium concentration ($[Ca^{2+}]_i$) was monitored by the fura-2 method described by Inoue et al. (1998), using a highly sensitive intensifier target video camera C2400 and an Argus 50 image processor (Hama-

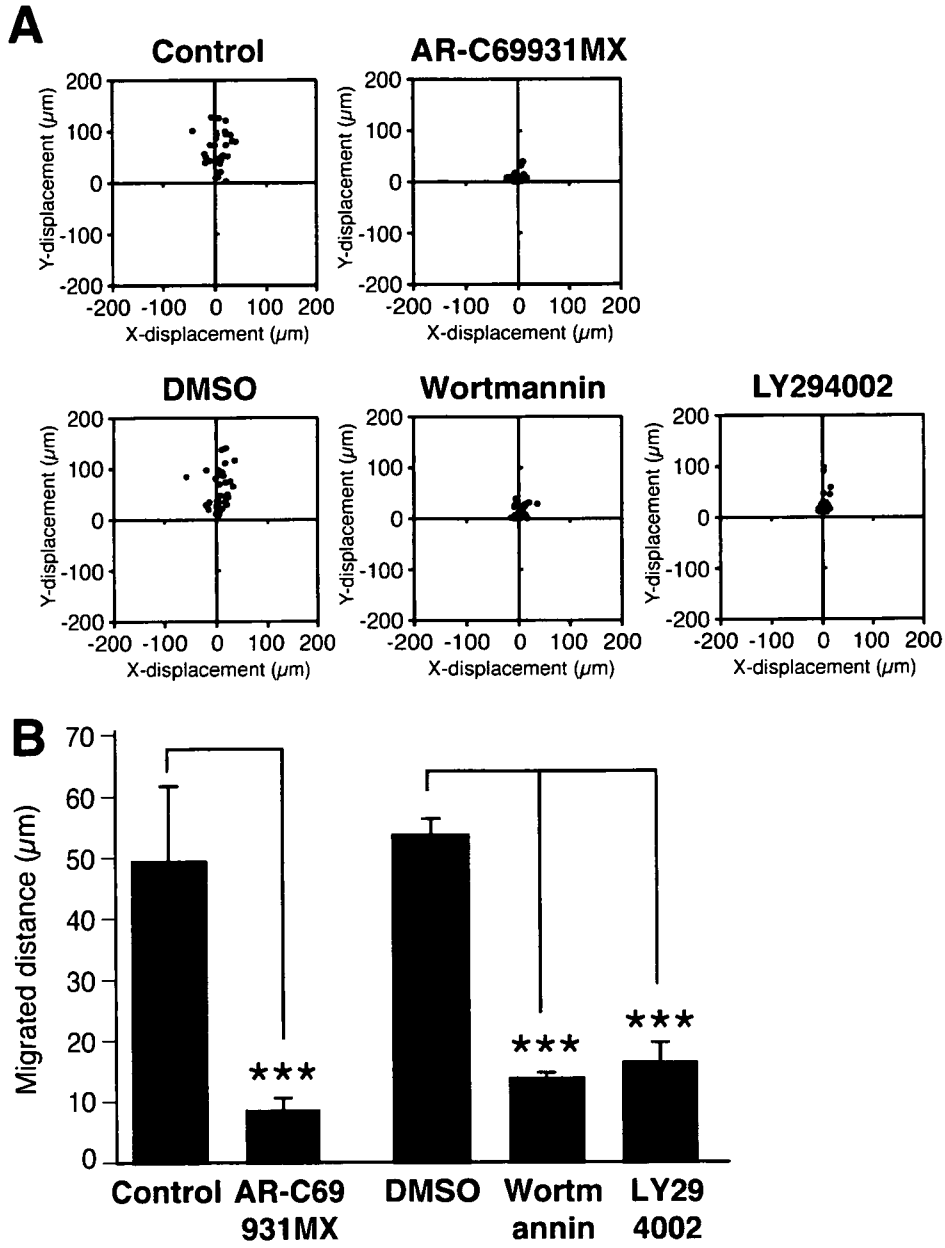

Fig. 1. Effect of PI3K inhibitors on ATP-induced microglial chemotaxis. (**A**) Microglia were pretreated with 1 μM AR-C69931MX for 10 min or with 0.125% DMSO, 100 nM wortmannin, or 50 μM LY294002 for 20 min, and microglial migration towards 50 μM ATP was observed in the Dunn chemotaxis chamber. The distance and direction migrated by individual cells are shown as x and y coordinates on scatter diagrams. The position of the outer well of the chamber is at the top in the vector diagrams of cells. (**B**) Chemotaxis by each cell was quantified by measuring the (x, y) distance migrated from the starting position. Data are means ± SD of three independent experiments. $^{***}P < 0.001$, Student's t-test.

matsu Photonics). Microglia transduced with the lentivirus vectors were plated at 2×10^5 cells/well on poly-L-lysine-coated CELLocate microgrid coverslips (Eppendorf, Hambrug, Germany). After 2 h, the cells were incubated with 10 μM fura-2 acetoxymethylester (fura-2/AM, Dojindo Laboratories, Kumamoto, Japan) at 37°C for 30 min in DMEM containing 25 mM HEPES (DMEM-H, Invitrogen), and the coverslips were mounted on an inverted epifluorescence microscope (TMD-300, Nikon, Tokyo, Japan). The cells were exposed to drugs dissolved in DMEM-H by superfusion. Raw data were recorded as 500-nm emissions of fura-2 excited alternately at 340 and 380 nm, and $[Ca^{2+}]_i$ was expressed as the ratio of the fluorescence intensity at 340 nm to the fluorescence intensity at 380 nm (F340/380).

RESULTS

Involvement of the PI3K Pathway in ATP-Induced Microglial Chemotaxis

We previously reported that ATP-induced microglial membrane ruffling were inhibited by treatment with pertussis toxin and a P2Y$_{12}$R-selective antagonist, AR-C69931MX, suggesting that Gi/o-coupled P2Y$_{12}$R is involved in both the membrane ruffling and the chemotaxis (Honda et al., 2001). Stimulation of P2Y$_{12}$R has been reported to induce PI3K activation (Czajkowski et al., 2004; Soulet et al., 2004; Van Kolen and Slegers, 2004). To determine whether PI3K activation is required for chemotaxis by ATP-stimulated microglia, we investigated the effects of the PI3K inhibitors wortmannin and

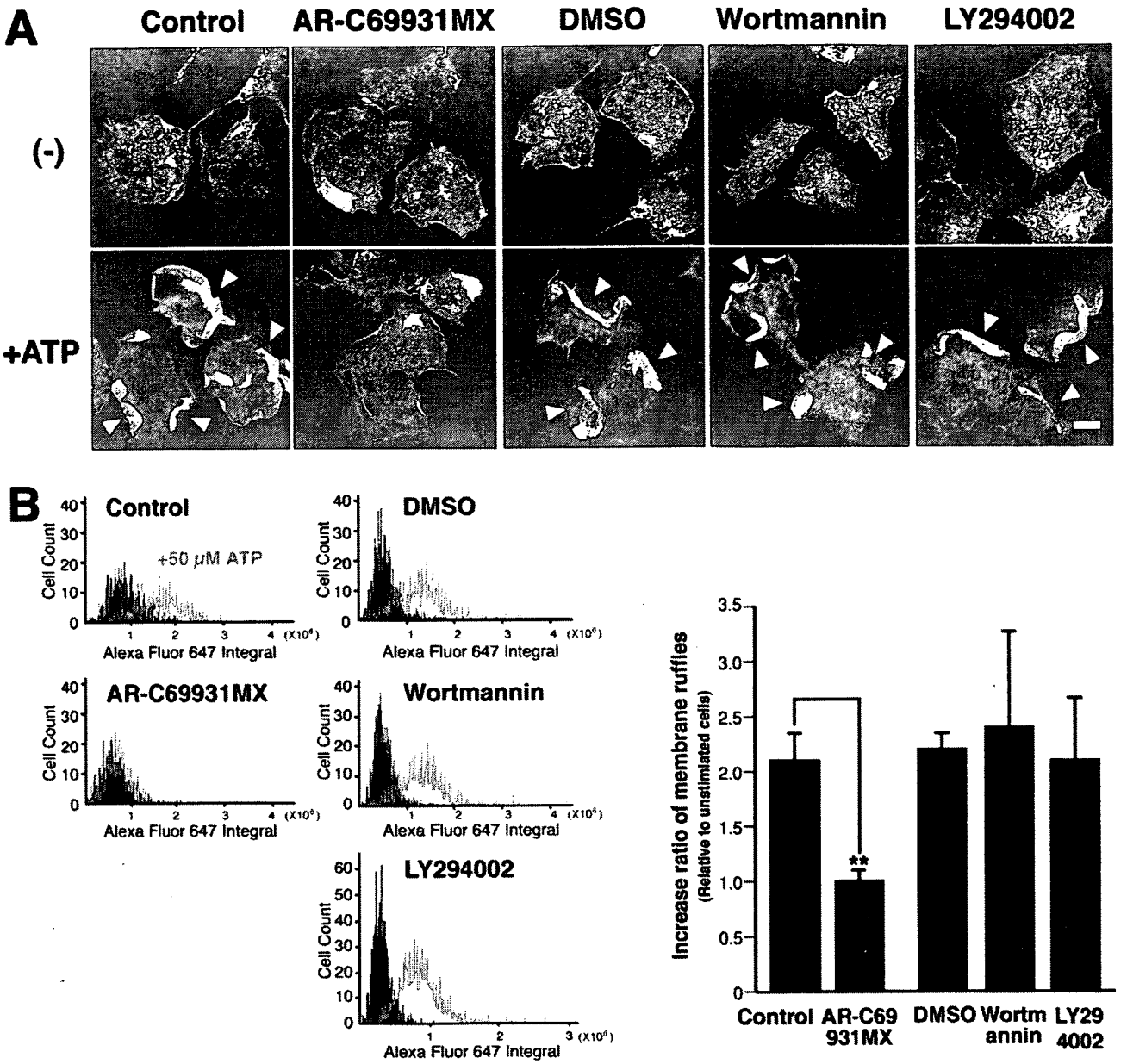

Fig. 2. Effect of PI3K inhibitors on ATP-induced microglial membrane ruffling. (**A**) Microglia were pretreated with 1 μM AR-C69931MX, 0.125% DMSO, 100 nM wortmannin, or 50 μM LY294002 as described in Fig. 1A, and then stimulated with 50 μM ATP for 5 min. After fixation, the cells were stained with Texas Red-conjugated phalloidin to visualize membrane ruffles. Arrowheads indicate membrane ruffles. Scale bar, 10 μm. (**B**) Quantification of membrane ruffles. Microglia were stimulated as in A for 5 min, fixed, and stained with an anti-Iba1 antibody and Alexa Fluor 647-conjugated phalloidin to recognize individual microglial cells and membrane ruffles, respectively. The F-actin content of microglial cells was quantified as integral intensity of Alexa Fluor 647 fluorescence by using LSC. The five panels on the left side are histograms representing the total F-actin in each cell (x-axis, Alexa fluor 647 integral) and the number of scanned cells (y-axis, cell count). The black region represents the unstimulated cells, and the region surrounded by the red line represents the ATP-stimulated cells. The bar graph on the right side shows the ratio of the mean of fluorescent intensity of ATP-stimulated cells to that of unstimulated cells after treatment with each inhibitor. Data are means ± SD of three independent experiments. $^{**}P < 0.01$, Student's t-test.

LY294002 with a Dunn chemotaxis chamber. Microglial chemotaxis toward the higher concentration of ATP was evaluated by analysis of time-lapse images. When 50 μM ATP was applied to the outer well, the cells migrated toward higher concentrations of ATP. Pretreatment of the microglia with wortmannin or LY294002 significantly blocked the chemotaxis (Fig. 1A). The chemotactic movement of the microglia was quantified by calculating the (x, y) distances individual cells migrated toward ATP. As shown in Fig. 1B, the mean distance migrated by cells pretreated with PI3K inhibitors was significantly shorter than the distance migrated by cells pretreated with DMSO. Treatment with 1 μM AR-C69931MX also inhibited the chemotaxis, as expected based on the results of our previous study (Honda et al., 2001). These findings suggested that PI3K activation is necessary for ATP-induced microglial chemotaxis.

Next, we investigated the effect of PI3K inhibitors on ATP-induced microglial membrane ruffling. As shown in Fig. 2A, phalloidin staining clearly demonstrated that ATP stimulation caused membrane ruffling within 5 min. Pretreatment of microglia with AR-C69931MX inhibited the ATP-induced membrane ruffling, as reported previously (Honda et al., 2001). However, exposure to 100 nM wortmannin or 50 μM LY294002 appeared to have no effect on the membrane ruffling. To confirm the effect of PI3K inhibitors on membrane ruffling quantitatively, the increase in F-actin in cells with membrane ruffles was analyzed with a laser scanning cytometer (LSC), which is a microscope-based cytometer. ATP-stimulated and unstimulated cells were stained with an anti-Iba1 antibody and Alexa Fluor 647-conjugatde phalloidin, and F-actin content was quantified by calculating the mean Alexa Fluor 647 fluorescent intensity of individual cells positive for a microglial marker protein Iba1 (Ito et al., 1998). As shown in Fig. 2B, the mean fluorescent intensity of control microglia was increased approximately 2-fold by ATP stimulation. The fluorescent intensity of ATP-stimulated cells pretreated with AR-C69931MX did not change significantly; however, the fluorescent intensity of cells pretreated with wortmannin or LY294002 was increased by ATP stimulation the same as in the control and the DMSO-treated cells. These results indicate that PI3K activation is not required for the membrane ruffling, but is necessary for induction of microglial chemotaxis.

ATP-Induced Akt Phosphorylation and Effect of Extracellular Calcium Deprivation

To determine whether the PI3K pathway in microglia is activated by ATP stimulation, we investigated Akt phosphorylation, a downstream signaling for PI3K (Bellacosa et al., 1991; Scheid and Woodgett, 2003), by Western blot analysis with a phospho-specific Akt antibody. ATP stimulation rapidly increased the level of Akt phosphorylation in a time-dependent manner (Fig. 3A), and pretreatment with 1 μM AR-C69931MX or 100 nM wortmannin inhibited the increase in Akt phosphorylation (Figs. 3B,C). These results indicated that ATP induces activation of the PI3K/Akt cascade in microglia and that the activation is mediated by P2Y$_{12}$R.

Previous studies (Inoue et al., 1998; Tsuda et al., 2003) have shown that stimulation of microglia with 50 μM ATP induces a transient increase in $[Ca^{2+}]_i$ that depends on the presence of extracellular Ca^{2+}, suggesting that ionotropic P2X receptors are responsible for the Ca^{2+} response. Use of the Ca^{2+}-sensitive fluorescent dye fura-2 revealed that the chelation of extracellular Ca^{2+} suppressed the ATP (50 μM)-evoked increase in $[Ca^{2+}]_i$ in our cultured microglia (data not shown). To determine whether the increase in $[Ca^{2+}]_i$ had any effect on the PI3K/Akt activation, we investigated Akt phosphorylation in microglia stimulated with 50 μM ATP in the absence of extracellular Ca^{2+}, and as shown in Fig. 4, chelation of extracellular Ca^{2+} by EGTA significantly

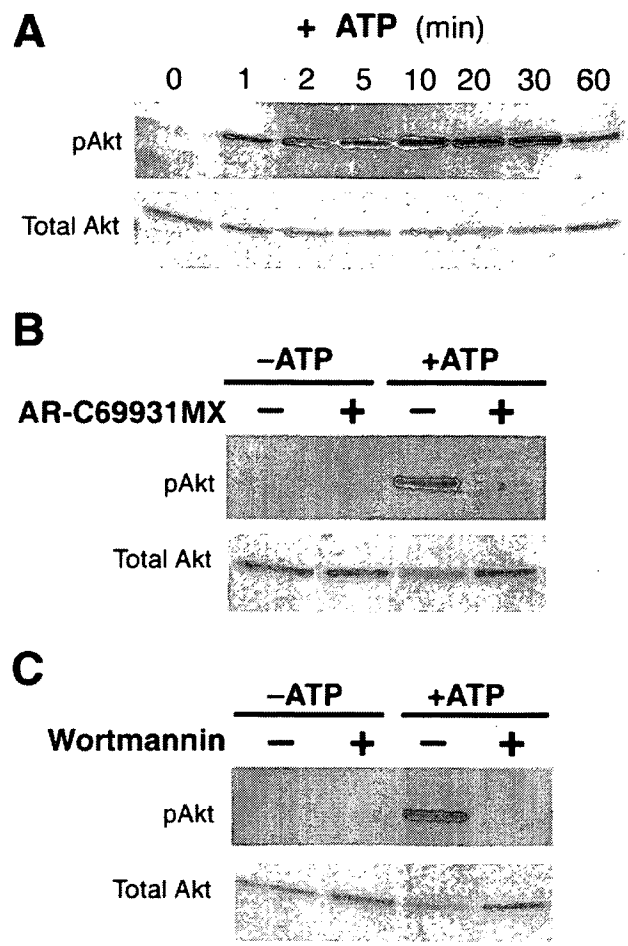

Fig. 3. ATP-induced Akt phosphorylation in microglia is dependent on PI3K activation through P2Y$_{12}$R. (**A**) Microglia were stimulated with 50 μM ATP for the period of time indicated and then lysed in SDS sample buffer. Phosphorylated (pAkt) and total Akt in the lysates were detected by Western blot analysis. (**B**, **C**) Microglia were pretreated with 1 μM AR-C69931MX for 10 min (**B**) or with 100 nM wortmannin for 20 min (**C**) and then stimulated with 50 μM ATP for 5 min. Akt phosphorylation was detected by Western blot analysis. Similar results were obtained from three independent experiments.

decreased ATP-induced Akt phosphorylation. Previous studies have shown that M-CSF stimulates the Fms tyrosine kinase receptor to activate Akt in macrophages in a PI3K-dependent manner (Comalada et al., 2004; Weiss-Haljiti et al., 2004). M-CSF also stimulated Akt phosphorylation in microglia, but chelation of extracellular Ca^{2+} had no effect on it (Fig. 4). These results led us to speculate that the ATP-induced PI3K/Akt activation, which is an essential component for induction of microglial chemotaxis, was linked to an increase in $[Ca^{2+}]_i$ through the extracellular Ca^{2+}-influx via ionotropic P2X receptors.

Effect of P2XR Antagonists on ATP-Induced Microglial Chemotaxis and Akt Phosphorylation

Since primary-cultured microglia have been shown to express P2X$_4$R (Tsuda et al., 2003; Xiang and Burnstock,

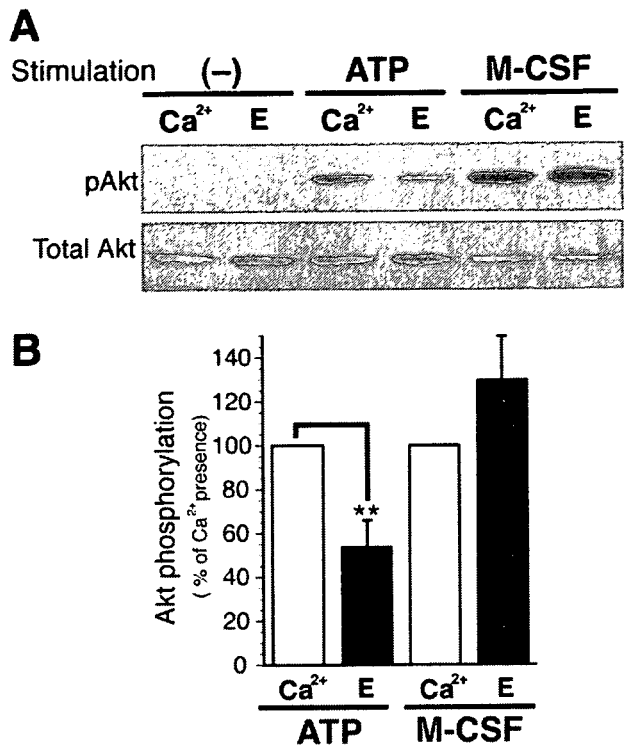

Fig. 4. Inhibitory effect of chelation of extracellular calcium on ATP-stimulated Akt phosphorylation. (**A**) Microglia were incubated for 30 min in BSS containing 1.2 mM Ca^{2+} (Ca^{2+}) or 1 mM EGTA (E) and then stimulated with 50 μM ATP or 100 ng/mL M-CSF for 5 min. Akt phosphorylation was detected by Western blot analysis. (**B**) The Akt phosphorylation level was quantified by densitometry. The results are expressed as percentage of agonist-induced phosphorylation in the presence of Ca^{2+} and are means ± SD of three independent experiments. $^{**}P < 0.01$; Student's *t*-test.

2005) and $P2X_7R$ (Ferrari et al., 1996; Nörenberg et al., 1994; Verkhratsky and Kettenmann, 1996; Walz et al., 1993), we first investigated the involvement of P2XRs in microglial chemotaxis with a $P2X_{1-4}R$, antagonist TNP-ATP, with a $P2X_{1,2,3,5,7}R$ antagonist PPADS, and with a selective $P2X_7R$ antagonist BBG. After pretreatment with an antagonist for 5 min the microglia were observed for chemotactic movement toward ATP in a Dunn chemotaxis chamber containing the antagonist. Treatment with 100 μM TNP-ATP appeared to suppress the ATP-induced microglial chemotaxis, but 300 μM PPADS or 1 μM BBG had no effect (Fig. 5A). The chemotactic movement of the microglia was quantified by calculating the mean value of the total (x, y) distances of individual cells migrated toward ATP. As shown in Fig. 5B, the mean distance migrated by the cells pretreated with TNP-ATP was significantly shorter than the distance migrated by the control cells, but the values of the cells pretreated with PPADS or BBG were not significantly different from those of the controls. Treatment with 1 μM AR-C69931MX also completely inhibited the chemotaxis. These results suggested that $P2X_4R$ as well as $P2Y_{12}R$ is involved in ATP-induced microglial chemotaxis.

We next examined the effect of the three P2XR antagonists, TNP-ATP, PPADS, and BBG, on ATP-stimulated Akt phosphorylation. TNP-ATP significantly suppressed the ATP-stimulated Akt phosphorylation, but PPADS or BBG appeared to have no effect (Fig. 6). AR-C69931MX also completely inhibited Akt phosphorylation. These results suggested that ATP-induced PI3K/Akt activation is mediated by $P2X_4R$ as well as $P2Y_{12}R$.

Downregulation of $P2X_4R$ in Microglia by Short Hairpin $P2X_4R$ RNAi

To determine whether $P2X_4R$ is in fact involved in ATP-induced microglial chemotaxis, we suppressed $P2X_4R$ expression in microglia with RNAi. We constructed a lentivirus vector that expresses both short hairpin (sh)-RNAi and EGFP under the control of the U6 RNA polymerase III promoter and the CMV promoter, respectively (Fig. 7A), and thus cells expressing the shRNAi should also express the EGFP reporter. Microglia were transduced with a lentivirus vector expressing a short hairpin $P2X_4R$ RNAi ($shP2X_4R$) or a control vector that expressed short hairpin luciferase RNAi (shControl). Lentiviral particles were added to mixed glial cell cultures, and floating cells were collected as microglia. To confirm the suppression of $P2X_4R$ expression by $shP2X_4R$, EGFP-positive cells were sorted with a flow cytometer, and expression of $P2X_4R$ protein in the cell lysate was investigated by Western blot analysis with an anti-$P2X_4R$ antibody. $P2X_4R$ protein expression was markedly suppressed in the EGFP-positive cells transduced with $shP2X_4R$ (Fig. 7B), whereas there was no difference in $P2X_4R$ protein level between the EGFP-positive and EGFP-negative cells after transduction with shControl. $P2X_7R$ protein expression was unaffected by transduction with $shP2X_4R$ (Fig. 7B). Microglial RNA was isolated from the sorted cells, and $P2Y_{12}R$ mRNA levels were analyzed by RT-PCR and normalized against actin mRNA levels. $P2Y_{12}R$ mRNA levels increased linearly with PCR reactions for 25–35 cycles. When PCR reactions were performed for 27 cycles, there was no difference in relative level of $P2Y_{12}R$ mRNA in EGFP-positive cells between transduction with $shP2X_4R$ and transduction with shControl (ratio of $P2Y_{12}R$ mRNA level in the $shP2X_4R$-transduced cells to the shControl-transduced cells = 1.1, Fig. 7C). We checked the $P2Y_{12}R$ mRNA level amplified by PCR for 25 and 30 cycles and confirmed that the relative level of $P2Y_{12}R$ mRNA in the $shP2X_4R$-transduced cells was the same as in the shControl-transduced cells. These results indicated that $P2X_4R$ expression was specifically suppressed in the EGFP-positive microglia after transduction with $shP2X_4R$.

The increase in $[Ca^{2+}]_i$ induced by ATP (50 μM) in microglia has been shown to be mediated by $P2X_4R$ (Tsuda et al., 2003). To determine whether $shP2X_4R$ interfered with $P2X_4R$ function in the EGFP-positive microglia, the level of $[Ca^{2+}]_i$ in individual cells was monitored by imaging analysis with fura-2 after transduction with the lentivirus vectors. A 30-s application of 50 μM ATP produced an increase in the 340/380 emission ratio of fura-2 in the EGFP-positive cells transduced with the con-

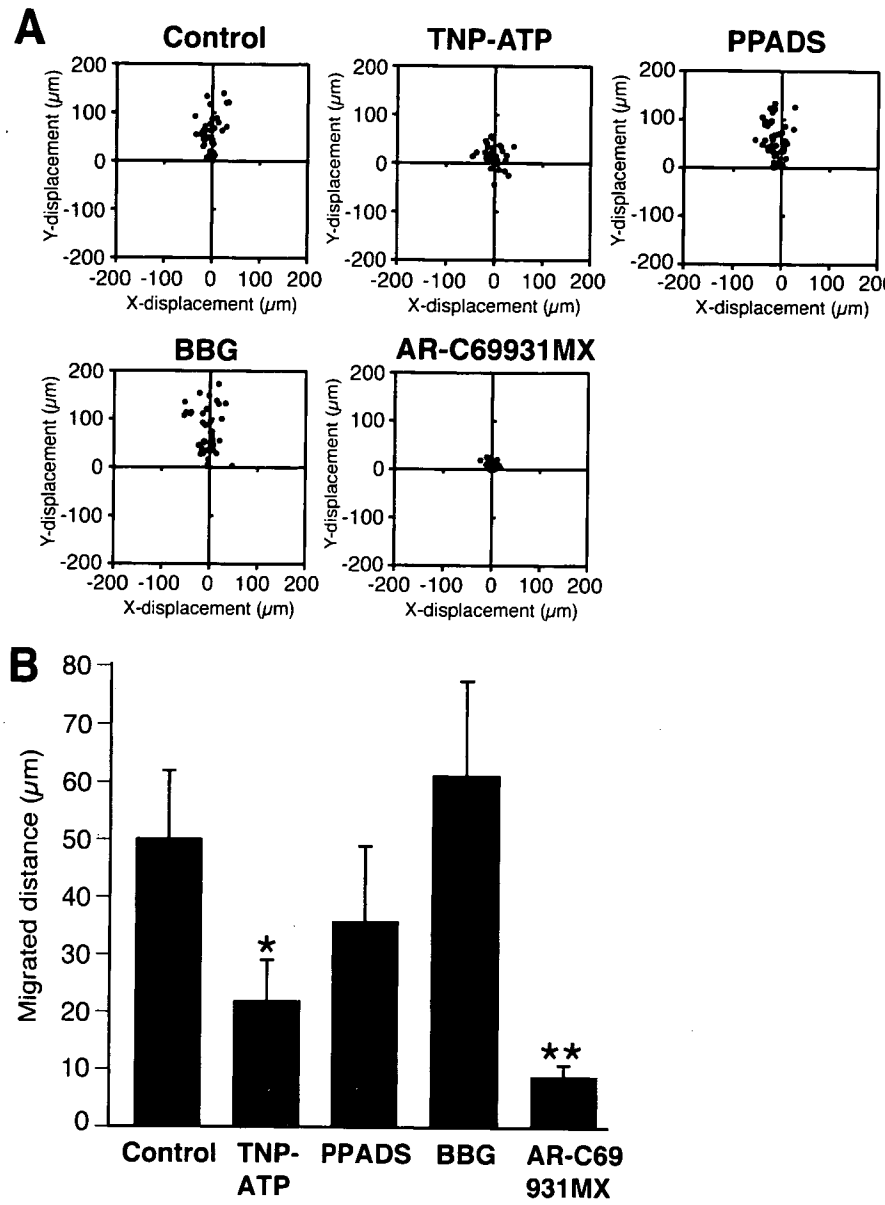

Fig. 5. Effect of P2X antagonists on ATP-induced microglial chemotaxis. (**A**) Microglia were pretreated with 100 μM TNP-ATP, 300 μM PPADS, or 1 μM BBG for 5 min or with 1 μM AR-C69931MX for 10 min. Microglial migration towards 50 μM ATP was observed in the Dunn chemotaxis chamber. The distance and direction of migration by individual cells are shown as x and y coordinates on scatter diagrams. (**B**) Chemotaxis was quantified by measuring the (x, y) distance migrated from the starting position of cells. Data are means ± SD of three independent experiments. $^{*}P < 0.05$, $^{**}P < 0.01$, Student's t-test.

trol vector (Fig. 8A left), whereas the increase in 340/380 emission ratio was significantly attenuated in the EGFP-positive cells transduced with shP2X$_4$R (Figs. 8A,B). These results confirmed that transduction with shP2X$_4$R downregulates expression of P2X$_4$R protein.

Effect of shP2X$_4$R on ATP-Induced Membrane Ruffling and Chemotaxis by Microglia

The effect of P2X$_4$R downregulation on ATP-induced membrane ruffling was examined in microglia transduced with the lentivirus vectors. EGFP-positive cells transduced with shP2X$_4$R or shControl developed membrane ruffles in response to ATP stimulation, the same as EGFP-negative cells (Fig. 9). These results indicated that shP2X$_4$R did not inhibit the activation of P2Y$_{12}$R and suggested that P2X$_4$R downregulation had no effect on ATP-induced membrane ruffling.

The cells transduced with the vectors were also examined for chemotactic movement in a Dunn chemotaxis chamber. As shown in the scatter diagrams, the migration of EGFP-positive cells transduced with shP2X$_4$R (Fig. 10A, bottom left) was clearly inhibited in comparison with the EGFP-negative cells (bottom right). EGFP-positive cells transduced with shControl (top left) migrated toward ATP as same as the EGFP-negative cells (top right). To quantify the effect of the shRNAi on the chemotactic movement of microglia, we calculated the mean value of the (x, y) distances EGFP-positive and -negative cells migrated toward ATP (Fig. 10B). The mean distance migrated by the EGFP-positive cells transduced with shP2X$_4$R was significantly shorter than both the mean distance migrated by the EGFP-negative cells and the mean distance migrated by the EGFP-positive cells

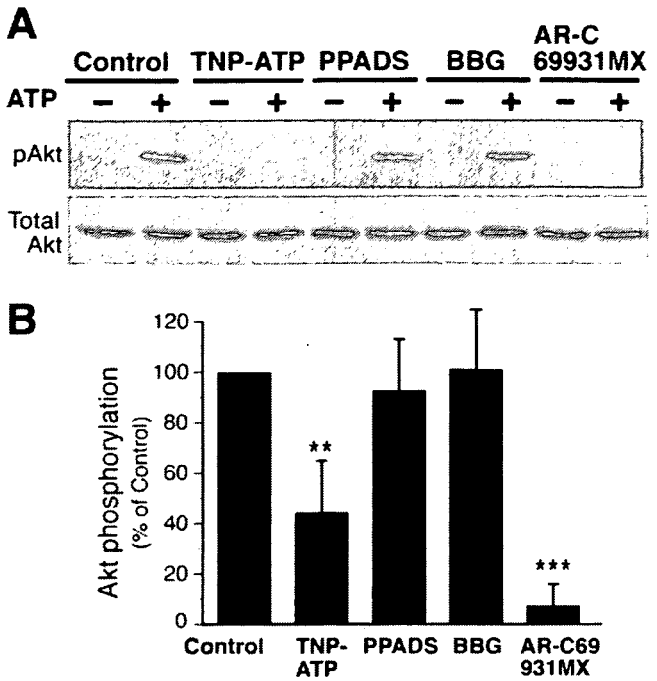

Fig. 6. Effect of P2X antagonists on ATP-stimulated Akt phosphorylation. (**A**) Microglia were pretreated with 100 μM TNP-ATP, 30 μM PPADS, or 100 nM BBG for 5 min or with 1 μM AR-C69931MX for 10 min, and then stimulated with 50 μM ATP for 5 min. Akt phosphorylation was detected by Western blot analysis. (**B**) The Akt phosphorylation level was quantified by densitometry and expressed as percentage of ATP-induced phosphorylation in control cells. The data shown are means ± SD of three independent experiments. $^{**}P < 0.01$, $^{***}P < 0.001$; Student's *t*-test.

transduced with shControl. There was no difference in distance migrated by the EGFP-positive cells and the EGFP-negative cells after transduction with shControl. These results clearly indicated that $P2X_4R$ is involved in ATP-induced microglial chemotaxis.

DISCUSSION

As expected from our previous findings (Honda et al., 2001), both the ATP-induced microglial membrane ruffling and chemotaxis were completely inhibited by a specific $P2Y_{12}R$ antagonist, AR-C69931MX, (Figs. 1 and 2). In this study we further investigated the signaling pathway downstream for $P2Y_{12}R$ and the effect of P2XR antagonists and shRNAi against $P2X_4R$ on microglial migration, and we found that $P2X_4R$ is also involved in ATP-induced microglial chemotaxis.

$P2Y_{12}R$ was known to be coupled to activation of PI3K and inhibition of adenylate cyclase (Czajkowski et al., 2004; Soulet et al., 2004; Van Kolen and Slegers, 2004), and Nasu-Tada et al. (2005) recently reported that a $P2Y_{12}R$-mediated decrease in cyclic AMP is an important step in membrane ruffling and chemotaxis by microglia on fibronectin-coated dishes. PI3K is well known to be a key player in remodeling of the actin cytoskeleton and in regulating cell migration, including chemotaxis (Procko and McColl, 2005; Van Haastert and Devreotes, 2004). In this study we showed that PI3K inhibitors

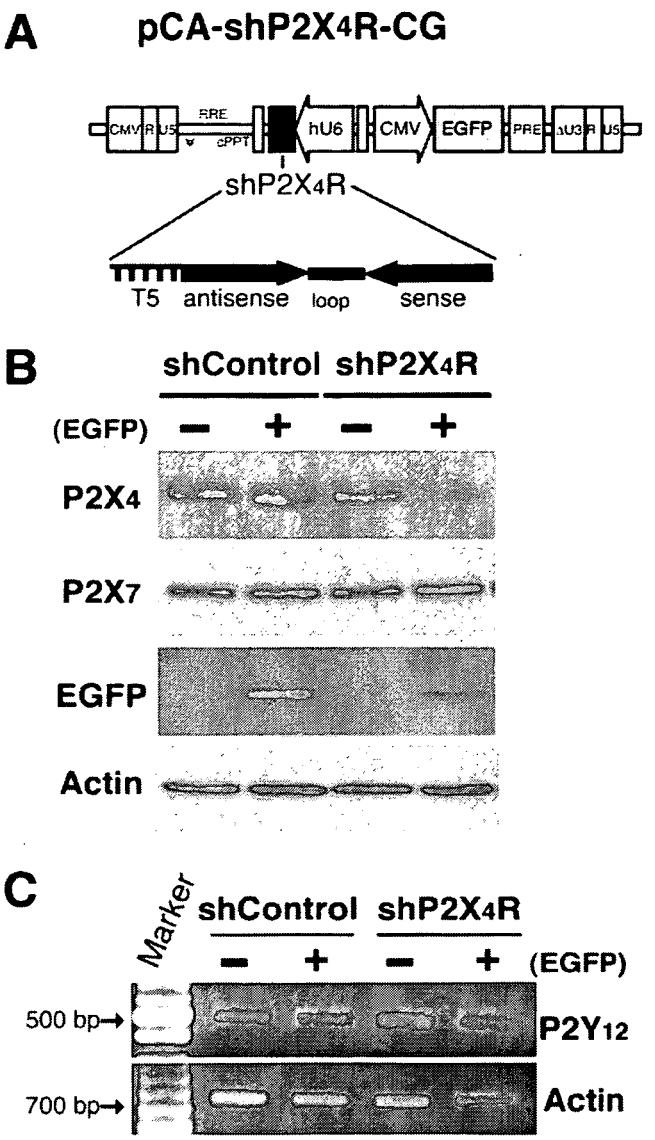

Fig. 7. shRNAi-targeted downregulation of $P2X_4R$ in microglia by lentivirus vectors. (**A**) Schematic drawing of lentivirus vectors expressing EGFP and shRNAi against $P2X_4R$ ($shP2X_4R$). A shRNA sequence targeted for firefly luciferase (shControl) was used as a control. (**B**) Protein expression of $P2X_4R$ and $P2X_7R$ in the microglia transduced with the shRNAi lentivirus vectors. EGFP-positive (+) and -negative (−) cells were sorted with a flow cytometer and lysed in SDS sample buffer. Protein expression of $P2X_4R$, $P2X_7R$, EGFP, and actin in the cell lysates was detected by Western blot analysis. Actin served as an internal control. (**C**) Gene transcript analysis of microglia transduced with the shControl or $shP2X_4R$ vector. RNA was isolated from the sorted cells. Gene transcripts for $P2Y_{12}R$ and β-actin, which served as an internal control, were analyzed by RT-PCR. The relative intensity of the bands for $P2Y_{12}R$ was quantified by densitometry and normalized to the β-actin products. Similar results were obtained from at least three independent experiments.

blocked microglial chemotaxis towards ATP (Fig. 1). However, the PI3K inhibitors had no effect on membrane ruffling (Fig. 2), suggesting that the initial actin reorganization induced by ATP is not dependent on PI3K activation, whereas the ATP gradient-dependent cell migration requires PI3K activation. PI3Ks phosphorylate phosphoinositides at the 3-hydroxyl of the inositol

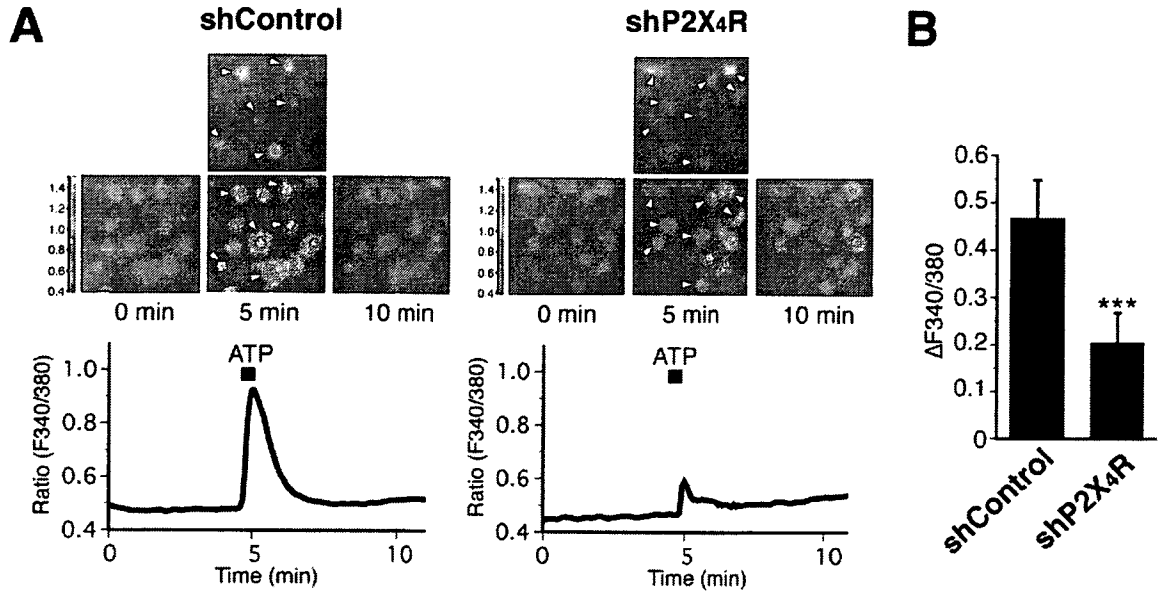

Fig. 8. Effect of P2X$_4$R downregulation on the ATP-evoked increase in $[Ca^{2+}]_i$ in microglia. (**A**) Microglia transduced with the shControl (left panel) or shP2X$_4$R (right panel) vector were loaded with fura-2/AM. $[Ca^{2+}]_i$ was expressed as the ratio of the fluorescence intensity at 340 nm to the fluorescence intensity at 380 nm (F340/380). The pseudocolor image shows three frames (0, 5, and 10 min) of fura2-loaded microglia stimulated with 50 μM ATP for 30 s. Arrowheads point to EGFP-positive cells. The traces show the mean increase in F340/380 emission ratio of 14 EGFP-positive cells from each culture. (**B**) The graphs show the relative increase in ratio (ΔF340/380; mean ± SD, n = 14 cells) from the basal level of the EGFP-positive cells shown in Fig. 8A. $^{***}P < 0.001$; Student's t-test. Similar results were obtained from three independent experiments.

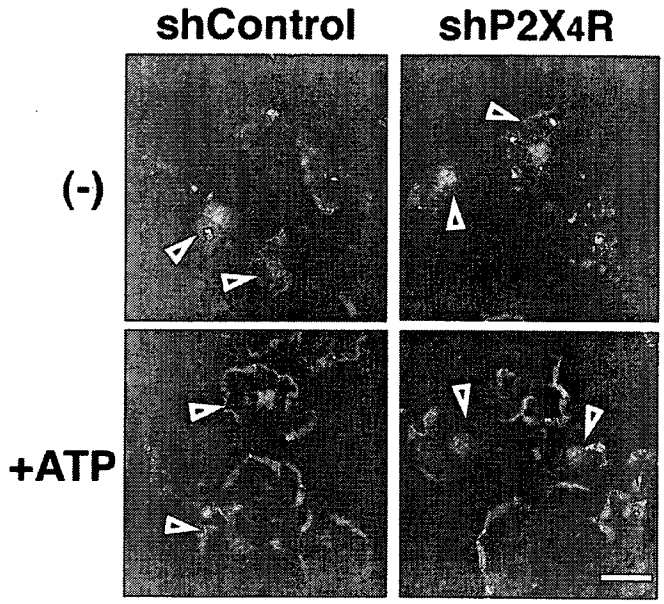

Fig. 9. Effect of P2X$_4$R downregulation on ATP-induced membrane ruffling of microglia. Microglia transduced with the lentivirus vectors were stimulated with 50 μM ATP for 5 min. After fixation, the cells were stained with Texas Red-conjugated phalloidin. Arrowheads indicate EGFP-positive cells. ATP-stimulated membrane ruffling of EGFP-positive cells were observed in three independent experiments. Scale bar, 20 μm.

ring (Vanhaesebroeck et al., 2001). When cells are placed in a chemoattractant gradient, the phosphorylated phospholipids selectively accumulate at the leading edge and act as a membrane anchor for many PI3K downstream effector proteins with pleckstrin homology (PH) regions, which may regulate directional sensing during chemotaxis (Procko and McColl, 2005; Van Haastert and Devreotes, 2004). PI3K will play a crucial role in both sensing the ATP gradient and determining the cell polarity of the microglia.

Akt is activated through binding of its PH domains to lipid products of PI3K on the plasma membrane (Scheid and Woodgett, 2003). In this study ATP-induced increase in Akt phosphorylation was suppressed by pretreatment with a P2Y$_{12}$R antagonist or PI3K inhibitors (Fig. 3). These findings indicated that Akt is phosphorylated following PI3K activation downstream of P2Y$_{12}$R in microglia. Interestingly, the increase in the Akt phosphorylation was suppressed by chelation of extracellular calcium with EGTA (Fig. 4), and depletion of intracellular calcium by BAPTA-AM also blocked the Akt phosphorylation (data not shown). These results indicate that activation of the PI3K-Akt signal pathway is regulated by an increase in $[Ca^{2+}]_i$. Previous studies have shown that in some cells an increase in $[Ca^{2+}]_i$ can activate Akt through PI3K-dependent or independent pathways. An increase in $[Ca^{2+}]_i$ can also activate Src or proline-rich/Ca^{2+}-activated tyrosine kinase Pyk2, thereby directly or indirectly regulating the PI3K activation (Chen et al., 2001; Gendron et al., 2003; Okuda et al., 1999). Protein kinase C (PKC) or Ca^{2+}/calmodulin-dependent protein kinase which is activated by calcium, lies upstream of Akt or directly phosphorylates Akt (Bauer et al., 2003; Gliki et al., 2002; Tanaka et al., 2003; Yano et al., 1998). Further investigation is needed to determine how the calcium signaling regulates the PI3K/Akt activation in microglia.

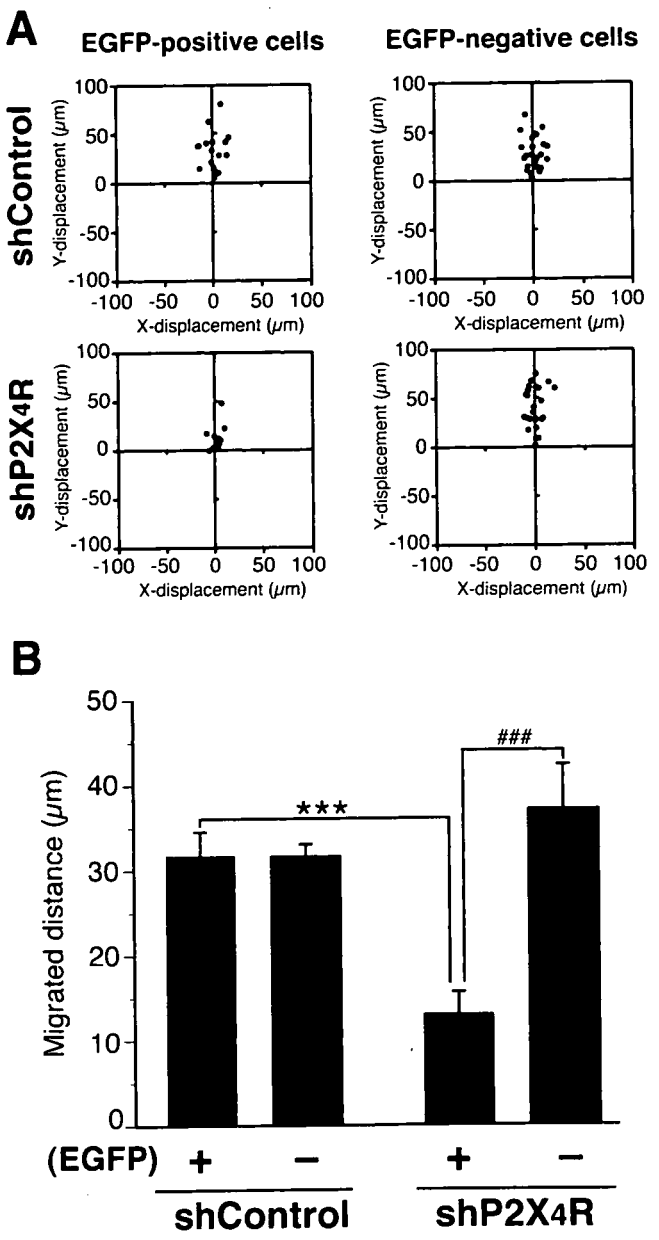

Fig. 10. Inhibitory effect of $P2X_4R$ downregulation on ATP-induced microglial chemotaxis. (**A**) Microglia were transduced with the lentivirus vectors and microglial migration towards 50 μM ATP was observed in the Dunn chemotaxis chamber. The distance and direction of movement by individual cells are shown as x and y coordinates on scatter diagrams. (**B**) Each chemotaxis was quantified by measuring the (x, y) distance migrated from the starting position of cells. Data are means ± SD of three independent experiments. $^{***}P < 0.001$, Student's t-test, compared with shControl EGFP-positive cells; $^{###}P < 0.001$, compared with shP2X4R EGFP-negative cells.

The ATP-induced increase in $[Ca^{2+}]_i$ in microglia has been shown to be suppressed by chelation of extracellular calcium or pretreatment with TNP-ATP, but not by PPADS or BBG (Tsuda et al., 2003). The present study showed that shRNA-mediated downregulation of $P2X_4R$ in microglia suppressed the ATP-induced increase in $[Ca^{2+}]_i$ (Fig. 8). These observations suggest that the increase in $[Ca^{2+}]_i$ is mainly caused by the influx of extracellular calcium through $P2X_4R$. ATP-induced PI3K/Akt activation was inhibited by pretreatment with TNP-ATP, but not with PPADS or BBG (Fig. 6). Interference with $P2X_4R$ expression markedly inhibited the ATP-induced microglial chemotaxis (Fig. 10) without affecting membrane ruffling (Fig. 9), the same as the effects of PI3K inhibitors (Figs. 1 and 2). We therefore suspect that the $P2X_4R$-mediated calcium signaling may be involved in PI3K/Akt activation and regulate microglial chemotaxis. Local Ca^{2+} mobilization through $P2X_4R$ at membrane ruffles may be necessary for maintenance or enhancement of the local $P2Y_{12}R$-activated PI3K signals.

Membrane ruffling is generated by dynamic remodeling of the actin cytoskeleton at the plasma membrane and is thought to be a crucial process for cell migration (Small et al., 2002). $P2Y_{12}R$ activation is essential for ATP-induced membrane ruffling and triggers intracellular signaling events that lead to microglial chemotaxis toward ATP. Ca^{2+} imaging showed that shP2×4R did not completely suppress the ATP-evoked increase in $[Ca^{2+}]_i$ (Fig. 9), suggesting that other subtypes of ATP receptor are involved in the Ca^{2+} response. P2Y receptors are generally linked to activation of phospholipase C (PLC) that catalyzes the hydrolysis of phosphatidylinositol 4,5-bisphosphate to the intracellular messenger inositol 1,4,5, triphosphate (IP_3) and diacylglycerol (Communi et al., 2000). ATP-stimulated $P2Y_{12}R$ will induce PLC activation, leading to IP_3-mediated Ca^{2+} release from intracellular calcium stores in microglia. P2Y receptors modulate G-protein coupled or voltage-dependent ion channels that affect the Ca^{2+} current (Van Kolen and Slegers, 2006). Vial et al. (2002) reported that coactivation of $P2X_1R$ and $P2Y_1R$ in platelets synergistically enhances the Ca^{2+} response and suggested that $P2X_1$ may have a priming role in the activation of $P2Y_1R$ during platelet activation. Further study is needed to analyze cross-talk between $P2X_4R$ and other signal pathways downstream of $P2Y_{12}R$, such as the adenylate cyclase pathway or PLC pathway.

$P2Y_{12}R$ is constitutively expressed in microglia in the normal brain (Sasaki et al., 2003). A recent report by Haynes et al. (2006) shows that $P2Y_{12}R$ is essential for early microglial responses towards either a local ATP injection or a focal laser injury in brain slices. $P2Y_{12}R$ play crucial roles in regulating the morphological changes in ramified microglia and cell migration by activated microglia in response to ATP released by surrounding cells and its hydrolysis product ADP. By contrast, $P2X_4R$ expression in microglia is lower in the normal brain and spinal cord, and it is significantly upregulated in activated microglia within 24 h after ischemia or nerve injury (Cavaliere et al., 2003; Schwab et al., 2005; Zhang et al., 2006). Tsuda et al. (2003) recently reported that the $P2X_4R$ expression is induced in spinal microglia during the tactile allodynia observed after nerve injury. These observations together with our own findings suggest that $P2X_4R$ activation may modulate or enhance the microglial cell migration in pathological conditions. Although further study is needed to clarify the molecular mechanisms underlying the microglial cell migration

mediated by $P2Y_{12}R$ and $P2X_4R$, the findings in the present study may contribute to understanding the ATP-induced changes in microglial dynamics in the brain in normal and pathological states.

ACKNOWLEDGMENTS

We thank Dr. Miyoshi (Bio Resource Center, RIKEN, Tsukuba, Japan) for providing us with lentivirus vector system, and Dr. Shin'ichi Takeda, Dr. Hirohiko Hojoh, and Mr. Masuda Satoshi (National Institute of Neuroscience) for their advice and technical support.

REFERENCES

Bauer B, Jenny M, Fresser F, Uberall F, Baier G. 2003. AKT1/PKBα is recruited to lipid rafts and activated downstream of PKC isotypes in CD3-induced T cell signaling. FEBS Lett 541:155–162.

Bellacosa A, Testa JR, Staal SP, Tsichlis PN. 1991. A retroviral oncogene, akt, encoding a serine–threonine kinase containing an SH2-like region. Science 254:274–277.

Cavaliere F, Florenzano F, Amadio S, Fusco FR, Viscomi MT, D'Ambrosi N, Vacca F, Sancesario G, Bernardi G, Molinari M, Volonte C. 2003. Up-regulation of $P2X_2$, $P2X_4$ receptor and ischemic cell death: Prevention by P2 antagonists. Neuroscience 120:85–98.

Chen R, Kim O, Yang J, Sato K, Eisenmann KM, McCarthy J, Chen H, Qiu Y. 2001. Regulation of Akt/PKB activation by tyrosine phosphorylation. J Biol Chem 276:31858–31862.

Comalada M, Xaus J, Sanchez E, Valledor AF, Celada A. 2004. Macrophage colony-stimulating factor-, granulocyte–macrophage colony-stimulating factor-, or IL-3-dependent survival of macrophages, but not proliferation, requires the expression of p21(Waf1) through the phosphatidylinositol 3-kinase/Akt pathway. Eur J Immunol 34:2257–2267.

Communi D, Janssens R, Suarez-Huerta N, Robaye B, Boeynaems JM. 2000. Advances in signalling by extracellular nucleotides. The role and transduction mechanisms of P2Y receptors. Cell Signal 12:351–360.

Czajkowski R, Banachewicz W, Ilnytska O, Drobot LB, Baranska J. 2004. Differential effects of $P2Y_1$ and $P2Y_{12}$ nucleotide receptors on ERK1/ERK2 and phosphatidylinositol 3-kinase signalling and cell proliferation in serum-deprived and nonstarved glioma C6 cells. Br J Pharmacol 141:497–507.

Davalos D, Grutzendler J, Yang G, Kim JV, Zuo Y, Jung S, Littman DR, Dustin ML, Gan WB. 2005. ATP mediates rapid microglial response to local brain injury in vivo. Nat Neurosci 8:752–758.

Ferrari D, Villalba M, Chiozzi P, Falzoni S, Ricciardi-Castagnoli P, Di Virgilio F. 1996. Mouse microglial cells express a plasma membrane pore gated by extracellular ATP. J Immunol 156:1531–1539.

Gendron FP, Neary JT, Theiss PM, Sun GY, Gonzalez FA, Weisman GA. 2003. Mechanisms of $P2X_7$ receptor-mediated ERK1/2 phosphorylation in human astrocytoma cells. Am J Physiol Cell Physiol 284: C571–C581.

Gliki G, Wheeler-Jones C, Zachary I. 2002. Vascular endothelial growth factor induces protein kinase C (PKC)-dependent Akt/PKB activation and phosphatidylinositol 3′-kinase-mediates PKC δ phosphorylation: Role of PKC in angiogenesis. Cell Biol Int 26:751–759.

Haynes SE, Hollopeter G, Yang G, Kurpius D, Dailey ME, Gan WB, Julius D. 2006. The P2Y(12) receptor regulates microglial activation by extracellular nucleotides. Nat Neurosci 12:1512–1519.

Honda S, Sasaki Y, Ohsawa K, Imai Y, Nakamura Y, Inoue K, Kohsaka S. 2001. Extracellular ATP or ADP induce chemotaxis of cultured microglia through Gi/o-coupled P2Y receptors. J Neurosci 21:1975–1982.

Illes P, Alexandre Ribeiro J. 2004. Molecular physiology of P2 receptors in the central nervous system. Eur J Pharmacol 483:5–17.

Imai Y, Ibata I, Ito D, Ohsawa K, Kohsaka S. 1996. A novel gene iba1 in the major histocompatibility complex class III region encoding an EF hand protein expressed in a monocytic lineage. Biochem Biophys Res Commun 224:855–862.

Inoue K. 2002. Microglial activation by purines and pyrimidines. Glia 40:156–163.

Inoue K, Nakajima K, Morimoto T, Kikuchi Y, Koizumi S, Illes P, Kohsaka S. 1998. ATP stimulation of Ca^{2+}-dependent plasminogen release from cultured microglia. Br J Pharmacol 123:1304–1310.

Ito D, Imai Y, Ohsawa K, Nakajima K, Fukuuchi Y, Kohsaka S. 1998. Microglia-specific localisation of a novel calcium binding protein, Iba1. Brain Res Mol Brain Res 57:1–9.

James G, Butt AM. 2002. P2Y and P2X purinoceptor mediated Ca^{2+} signalling in glial cell pathology in the central nervous system. Eur J Pharmacol 447:247–260.

Kreutzberg GW. 1996. Microglia: A sensor for pathological events in the CNS. Trends Neurosci 19:312–318.

Moran LB, Graeber MB. 2004. The facial nerve axotomy model. Brain Res Brain Res Rev 44:154–178.

Nakajima K, Kohsaka S. 2005.Response of microglia to brain injury. In: Kettenmann H, Ransom BR, editors. Neuroglia. New York: Oxford University Press. pp 443–453.

Nakajima K, Shimojo M, Hamanoue M, Ishiura S, Sugita H, Kohsaka S. 1992. Identification of elastase as a secretory protease from cultured rat microglia. J Neurochem 58:1401–1408.

Nasu-Tada K, Koizumi S, Inoue K. 2005. Involvement of β1 integrin in microglial chemotaxis and proliferation on fibronectin: Different regulations by ADP through PKA. Glia 52:98–107.

Nimmerjahn A, Kirchhoff F, Helmchen F. 2005. Resting microglial cells are highly dynamic surveillants of brain parenchyma in vivo. Science 308:1314–1318.

Nishitsuji H, Ikeda T, Miyoshi H, Ohashi T, Kannagi M, Masuda T. 2004. Expression of small hairpin RNA by lentivirus-based vector confers efficient and stable gene-suppression of HIV-1 on human cells including primary non-dividing cells. Microbes Infect 6: 76–85.

Nörenberg W, Langosch JM, Gebicke-Haerter PJ, Illes P. 1994. Characterization and possible function of adenosine 5′-triphosphate receptors in activated rat microglia. Br J Pharmacol 111:942–950.

Okuda M, Takahashi M, Suero J, Murry CE, Traub O, Kawakatsu H, Berk BC. 1999. Shear stress stimulation of p130(cas) tyrosine phosphorylation requires calcium-dependent c-Src activation. J Biol Chem 274:26803–26809.

Procko E, McColl SR. 2005. Leukocytes on the move with phosphoinositide 3-kinase and its downstream effectors. Bioessays 27:153–163.

Ralevic V, Burnstock G. 1998. Receptors for purines and pyrimidines. Pharmacol Rev 50:413–492.

Ridley AJ. 2001. Rho proteins, PI 3-kinases, and monocyte/macrophage motility. FEBS Lett 498:168–171.

Sasaki Y, Hoshi M, Akazawa C, Nakamura Y, Tsuzuki H, Inoue K, Kohsaka S. 2003. Selective expression of Gi/o-coupled ATP receptor $P2Y_{12}$ in microglia in rat brain. Glia 44:242–250.

Scheid MP, Woodgett JR. 2003. Unravelling the activation mechanisms of protein kinase B/Akt. FEBS Lett 546:108–112.

Schwab JM, Guo L, Schluesener HJ. 2005. Spinal cord injury induces early and persistent lesional $P2X_4$ receptor expression. J Neuroimmunol 163:185–189.

Small JV, Stradal T, Vignal E, Rottner K. 2002. The lamellipodium: Where motility begins. Trends Cell Biol 12:112–120.

Soulet C, Sauzeau V, Plantavid M, Herbert JM, Pacaud P, Payrastre B, Savi P. 2004. Gi-dependent and -independent mechanisms downstream of the $P2Y_{12}$ ADP-receptor. J Thromb Haemost 2:135–146.

Stence N, Waite M, Dailey ME. 2001. Dynamics of microglial activation: A confocal time-lapse analysis in hippocampal slices. Glia 33:256–266.

Streit WJ. 2002. Microglia as neuroprotective, immunocompetent cells of the CNS. Glia 40:133–139.

Tanaka Y, Gavrielides MV, Mitsuuchi Y, Fujii T, Kazanietz MG. 2003. Protein kinase C promotes apoptosis in LNCaP prostate cancer cells through activation of p38 MAPK and inhibition of the Akt survival pathway. J Biol Chem 278:33753–33762.

Tsuda M, Shigemoto-Mogami Y, Koizumi S, Mizokoshi A, Kohsaka S, Salter MW, Inoue K. 2003. $P2X_4$ receptors induced in spinal microglia gate tactile allodynia after nerve injury. Nature 424:778–783.

Van Haastert PJ, Devreotes PN. 2004. Chemotaxis: Signalling the way forward. Nat Rev Mol Cell Biol 5:626–634.

Vanhaesebroeck B, Leevers SJ, Ahmadi K, Timms J, Katso R, Driscoll PC, Woscholski R, Parker PJ, Waterfield MD. 2001. Synthesis and function of 3-phosphorylated inositol lipids. Annu Rev Biochem 70:535–602.

Van Kolen K, Slegers H. 2004. $P2Y_{12}$ receptor stimulation inhibits β-adrenergic receptor-induced differentiation by reversing the cyclic AMP-dependent inhibition of protein kinase B. J Neurochem 89:442–453.

Van Kolen K, Slegers H. 2006. Integration of P2Y receptor-activated signal transduction pathways in G protein-dependent signaling networks. Purinergic Signalling 2:451–469.

Vial C, Rolf MG, Mahaut-Smith MP, Evans RJ. 2002. A study of P2X1 receptor function in murine megakaryocytes and human platelets reveals synergy with P2Y receptors. Br J Pharmacol 135:363–372.

Verkhratsky A, Kettenmann H. 1996. Calcium signalling in glial cells. Trends Neurosci 19:346–352.